Bringing It Indoors: A Review of Narrowband Radio Propagation Modeling for Enclosed Spaces

MELISSA EUGENIA DIAGO-MOSQUERA [1], **ALEJANDRO ARAGÓN-ZAVALA**[1], **AND GERARDO CASTAÑÓN**[2]

[1]Computing Department, School of Engineering and Science, Tecnológico de Monterrey, Querétaro 76130, Mexico
[2]Department of Electrical and Computing Engineering, Tecnológico de Monterrey, Monterrey 64849, Mexico

Corresponding author: Melissa Eugenia Diago-Mosquera (a00829220@itesm.mx)

ABSTRACT Small cells are now widely deployed indoors to address hot-spot areas where capacity uplift is needed. This deployment leads to the increase of wireless networks as a challenge to service demands of personal communication systems, which has inspired the scientific community to work towards understanding and predicting in-building radio wave propagation performance. Despite this, only a few reviews have attempted to overview channel modeling for specific indoor environments and even fewer outline remarks that include a methodology for designing and planning indoor radio systems. Consequently, a comprehensive survey of indoor narrowband channel models is presented, spanning more than 30 years of continuous research to overview and contrast significant developments including their disadvantages, and proposing a new taxonomy to analyze them. Finally, remarks on indoor radio propagation modeling with a vision for future research opportunities are presented.

INDEX TERMS Indoor channel models, indoor radio wave propagation, wireless propagation.

I. INTRODUCTION

The widespread use of mobile communications, since its initial implementation in the early 1980s, has led not only to an increasing wealth of this technology but also to a reasonable increase in grade of service (GoS) demands of mobile users, thereby stressing the coverage to handle more users with heterogeneous GoS levels. According to the Cisco Visual Networking Index (VNI) report published in [1], by 2022, global mobile devices will grow from 8.6 billion in 2017 to 12.3 billion by 2022.

Considering the challenges of this explosive growth and the fact that people (mobile network subscribers initially), on average—according to the United States Environmental Protection Agency, EPA—spend approximately 90% of their time indoors [2], in-building wireless performance takes a fundamental place on network operation management for allowing coverage all the time, everywhere. The adaptation of this mobile technology to in-building scenarios is what makes it flexible and robust, responding to the changing needs

of people and businesses to deliver a satisfactory in-building experience to mobile users.

From the early stages of 5G planning to the detailed evolution of 5G requirements, it has been clear that small cells are a key component for making the path to 5G practical and profitable. A small cell is a radio access point with low radio frequency power output, footprint and range. It is operator-controlled and can be deployed indoors or outdoors. Small cells complement the macro network to improve coverage, add targeted capacity, and support new services while improving user experience [3].

In order to deliver higher quality to mobile users inside buildings, small cells have been deployed to address hot-spot areas where an increase in capacity is needed. This has led to a growing interest among wireless engineers for understanding and predicting how radio waves propagate inside buildings and other enclosed spaces. As this rise of mobile communications continues, it is valuable to have processes and methodologies that can provide a high level of confidence in the design of indoor radio propagation systems. Therefore, it is important to explore in-building mathematical propagation models with a high degree of accuracy, understanding how wireless signals are affected over distance due to wall

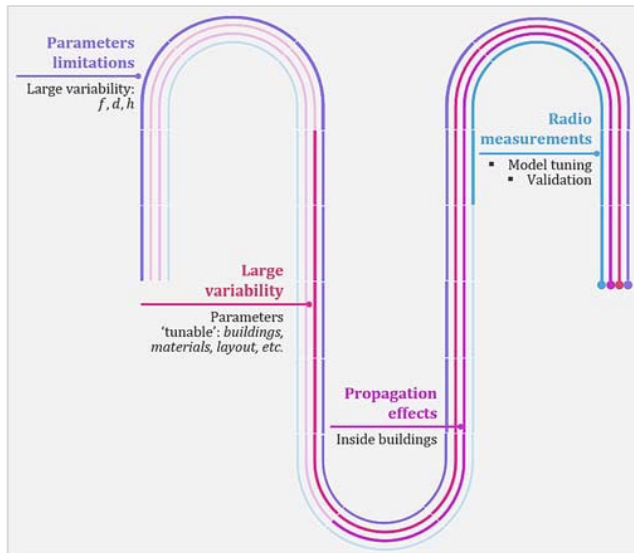The associate editor coordinating the review of this manuscript and approving it for publication was Jiayi Zhang [ID].

FIGURE 1. Propagation modeling challenges.

and floor penetration losses and multipath effects. Some key points that outline the importance of accurate channel modeling are:

- The in-building radio propagation phenomena, complex by nature, can be characterized with appropriate channel models that include key propagation effects.
- The range of a wireless communication system can be estimated assessing the expected coverage—path loss map—inside a building, including potential antenna locations and their expected coverage range.
- Signal strength/path loss can be predicted more accurately everywhere in a building or enclosed space.
- Channel performance predictions can be made quickly, e.g., signal-to-noise ratio (SNR), received signal power, carrier-to-interference ratio (C/I), etc.
- Signal strength predictions can be useful for areas where measurements cannot be made.

Propagation modeling challenges are shown Fig. 1, according to Aragòn-Zavala [4, Ch. 5]. For indoor deployments, the following challenges are identified:

- Parameter limitations—approximations that are necessary to describe a system using mathematical concepts within a computational development—due to the large variability that exists in indoor radio propagation.
- Model parameter calibration that depends on specific building characteristics that otherwise could not be modeled.
- High complexity in considering propagation effects inside buildings, having in mind that in many cases it is hard to separate them and characterize those individually.
- Conditions under which radio measurements were performed at different times. Since measurements are used for both model tuning and validation, it is expected to have a scenario under similar conditions.

A. RELATED LITERATURE REVIEWS PUBLISHED

In 2002, Iskander and Yun [5] focused on deterministic prediction models for path loss based on ray-tracing techniques. The authors briefly discussed efforts to characterize walls of complex structures and develop equivalent ray-tracing models for windows and metal-framed structures, considering venues such as office and factory buildings. One year later, Sarkar *et al.* [6] reviewed available information on various propagation models for both indoor and outdoor. They highlighted that the distance/power model is the main propagation modeling approach for path loss, adding wall and floor attenuation factors to the path loss computation.

Later, in 2008, Anusuya *et al.* [7] surveyed different channel models used to characterize indoor wireless systems, and they concluded that the efficiency of a model is measured by computational complexity whereas its accuracy can be measured by estimating its prediction error. In contrast, Neskovic *et al.* [8] mentioned that in order to increase system efficiency, mutual interference should be avoided, thus favoring coexistence as a result of suitable techniques for the prediction of indoor electromagnetic propagation.

By 2009, Neskovic *et al.* [8] and Trinchero and Stefanelli [9] focused their works on analyzing the technical literature to summarize and classify the most important methods for the prediction of electromagnetic propagation inside buildings. Smulders [10] addressed the statistical characterization—one of the classifications made by Neskovic *et al.*—of indoor radio channels operating in the 60 GHz frequency band. Phillips *et al.* [11] reviewed path loss prediction methods, works from 1940 to 2013, although not focusing on indoor environments but subdividing the models into apriori (six categories) and active measurement models (four categories).

Considering that underground mines and tunnels are enclosed spaces, Forooshani *et al.* in 2013 [12] and Hrovat *et al.* in 2014 [13], focused their surveys on these approaches, highlighting the implications of the physical environment (thick concrete walls), antenna placement and radiation characteristics on wireless communication system design.

In the review paper presented by Deb *et al.* in 2017 [14], different path loss models are discussed for indoor femtocells, assuming that the mobile users in that region exclusively access services delivered by femtocells. Additionally, the authors performed a comparative analysis of indoor path loss models at 2 GHz, where they considered the effect of two types of walls: light walls made of glass, plastic, etc. and heavy walls made of concrete and brick. They concluded that the most suitable in-building path loss model could be selected depending on frequency range, building structure, and wall and floor type.

To summarize this section, a survey of model classification and important annotations reported in the literature is given in Table 1.

The related works in Table 1 agree with the idea that at a specific location, the signal path for indoor environments is created by a much larger number of indirect components than

TABLE 1. Propagation model classification.

Review	Propagation model classification		Scenario	Contributions

Iskander & Yun, 2002 [5]	1. Deterministic
	  1.1. Empirical
	  1.2. Theoretical
	  1.3. Site-specific
		2. Statistical	Terrestrial wireless communication systems	Schemes to increase computational efficiency and accuracy are discussed.

Sarkar et al., 2003 [6]	1. Empirical (statistical)	2. Site-specific (deterministic)	Indoor and outdoor environments	An impulse response characterization for the propagation path is presented.
Anusuya et al., 2008 [7]	1. Deterministic	2. Statistical 3. Site-specific	Wireless indoor environment	-
Neskovic et al., 2009 [8]	1. Statistical (empirical)	2. Theoretical	Macrocell, microcell and indoor wireless communication channels	Advantages and disadvantages are discussed.

Trinchero & Stefanelli, 2009 [9]	1. Deterministic
	  1.1. Ray methods
	  1.2. Integral methods
	  1.3. Differential equation methods
		2. Heuristic
		  2.1. Empirical models.
		  2.2. Statistical models.
		3. Hybrid
			Indoor environment	-

Phillips et al., 2013 [11]	1. Apriori
	  1.1. Theoretical/Foundational Models
	  1.2. Basic Models
	  1.3. Terrain Models
	  1.4. Supplementary Models
	  1.5. Stochastic Fading Models
	  1.6. Many-Ray Models
		2. Active measurement
		  2.1. Explicit mapping
		  2.2. Partition models
		  2.3. Iterative Heuristic Refinement
		  2.4. Active Learning and Geostatistics
			Wireless communication systems	▪ Period of more than 60 years was covered.
				▪ New taxonomy for path loss models.

Forooshani et al., 2013 [12]	1. Theoretical	2. Measurement-based	Underground mines	Period from 1920 to 2012.
Hrovat et al., 2014 [13]	1. Empirical	2. Deterministic	Tunnels	-
Deb et al., 2017 [14]	1. Empirical (statistical)	2. Semi-Empirical (theoretical)	Indoor environment covered by femtocell	Comparative analysis between: COST 231, MWF, WINNER II NLOS and ITU-R P models.

Hemadeh et al., 2018 [15]	2. Physical
	  2.1. Deterministic
	  2.2. Stochastic
		3. Analytical
		  3.1. Propagation-based
		  3.2. Correlation-based
			Millimeter wave wireless communication systems	▪ Frequency bands: 28, 38, 60 and 73 GHz.
				▪ Measurement campaigns are conducted.

in the case of an outdoor environment. Therefore, the indoor signal level is more fluctuating than the outdoor one, and thus, more difficult to predict. Multipath results from multiple reflections caused by obstacles and is more severe inside buildings. The received signal arrives as a random and unpredictable set of reflections and/or direct waves, each one with its own degree of attenuation, phase and delay. Consequently, multipath leads to variations in the received signal strength over frequency and antenna location.

Phillips *et al.* [11] believe that measurement-based methods and rigorous—comparative—validation are needed; moreover, that the future of wireless path loss prediction will be active measurement designs that attempt to extract information from measurements and not only from theoretical predictions. In particular, geostatistical approaches that favor robust sampling designs and explicitly model the spatial structure of measurements are mentioned to be promising.

Additionally, Phillips *et al.* [11] state that theoretical models provide valuable physical insights about electromagnetic propagation. However, since most of these models are based on non-realistic assumptions, they need to be evaluated through experiments. Although the cost and effort for

conducting measurements increase in complex environments, the measurement-based approach has proven to be useful and productive.

B. PAPER OUTLINE

This paper provides a comprehensive survey of indoor channel models found in the literature, spanning more than 30 years of continuous research. The objectives of this survey are:

- to introduce the main propagation characteristics for wireless communications in indoor scenarios;
- to survey the available in-building mathematical models in the literature and propose a new taxonomy to analyze them, providing a complete and updated overview; and
- to outline remarks for indoor radio propagation modeling.

The remainder of this paper is organized as follows, noting that the reviewed literature is limited to narrowband systems. In Section II, the main theory to study the indoor propagation phenomena is covered. A thorough explanation and review of in-building radio wave propagation models is presented in Section III, as well as a new classification for indoor path

loss models is introduced. Concluding remarks are presented in Section IV. Finally, in section V, research opportunities and future developments are discussed.

II. INDOOR RADIO WAVE PROPAGATION

In order to understand the nature of the models that will be presented, several definitions need to be highlighted, underlying the theory that introduces the basic concepts of indoor radio propagation.

A. PATH LOSS AND PROPAGATION MECHANISMS

The path loss between a pair of antennas is the ratio of the transmitted power to the received power, usually expressed in decibels. It includes all the possible elements of loss associated with interactions between the propagating wave and any objects between transmitting and receiving antennas. As a result of radio wave propagation over a channel, the radio signal is attenuated due to path loss, as well as fading processes occur [16].

The basic components for performing an analysis of a wireless communication system are illustrated in Fig. 2 (considering the losses and gains in the system). In order to quantify link performance, a link budget of the system is required, taking into account the basic elements shown in Fig. 2.
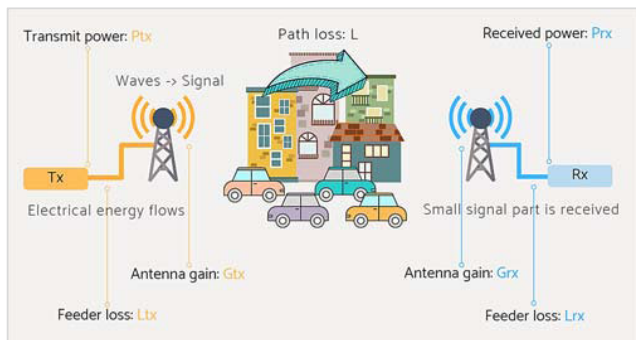

FIGURE 2. Elements of a wireless communication system.

The mechanisms behind electromagnetic wave propagation are diverse but can generally be attributed to: reflection, refraction, diffraction and scattering [17, Ch. 3]. The path between transmitter and receiver inside buildings can be either line-of-sight (LOS) or non-line-of-sight (NLOS). When radio systems do not have a LOS path and the presence of walls and floors causes severe diffraction loss and multiple reflections from various objects, the electromagnetic waves travel along different paths of varying lengths. The interaction between these waves causes multipath fading at a specific location, and field strength decrease as the distance between the transmitter and receiver increases.

1) REFLECTION, REFRACTION AND DIFFRACTION

When a propagating electromagnetic wave impinges upon an object that has very large dimensions compared to the wavelength of the propagating wave, reflection and refraction occur (illustrated in Fig. 3). As a result, two new waves are produced, each with the same frequency as the incident wave.
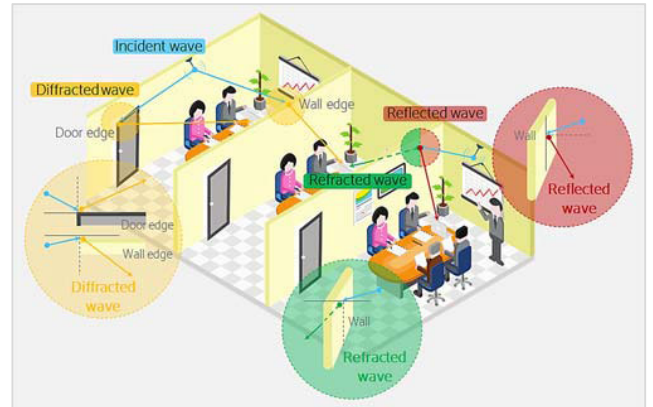

FIGURE 3. Propagation mechanisms: Reflection, refraction and diffraction.

The reflected wave arises from the surface of the floor and roof, from walls, windows and furniture in an enclosed space.

When reflection occurs, the wave may also be partially refracted. Reflection and refraction coefficients are functions of the material properties of the medium and generally depend on wave polarization, angle of incidence and frequency of the propagating wave.

Wall and floor materials have a strong influence on the propagation losses and, thus, in the amount of signal that can be received after going deeper into a building as a result of refraction.

In NLOS propagation, a signal transmitted through a wireless medium reaches the receiver via one or more indirect paths, each having different attenuations and delays. NLOS propagation is responsible for coverage behind walls and other obstructions inside buildings—shadow regions—and this is possible thanks to diffraction that occurs when the radio path between the transmitter and receiver is obstructed by a surface with sharp edges, i.e., a door or a wall edge represented in Fig. 3. The waves produced by the obstructing surface are present throughout space and even behind the obstacle, giving rise to propagation into the shadow region.

2) SCATTERING

Similar to reflection, scattering occurs when the wave is reflected, but in this case, the surface consists of irregularities with dimensions that are smaller compared to the signal wavelength and where the number of obstacles per volume unit is large, such as a rough surface like the one shown in Fig. 4. Therefore, the reflected wave becomes scattered from many positions on the surface, broadening the scattered energy [4, Ch. 4], and it increases the energy radiated in other directions. Scattering can become much more significant as frequency increases, such as in the millimeter-wave band for 5G.

3) WAVEGUIDING

This effect is the result of reflections and refractions given in areas such as corridors or other narrow gaps between walls, which wind up carrying the wave along the waveguide to
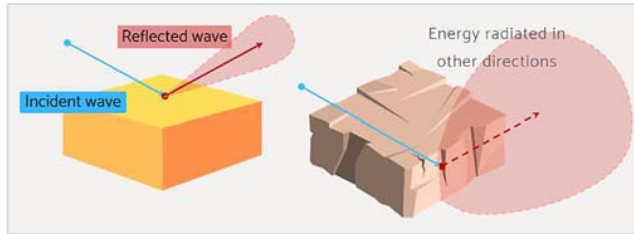
FIGURE 4. Scattering: rough surface.

the receiver. Waveguiding depends on incident angles, material types and distances between walls, and it produces the so-called waveguiding gain [4, Ch. 4], increasing penetration depth along corridors.

In [18], parameters affecting large-scale path loss including waveguiding were analyzed. Under certain conditions, stronger constructive interference can be produced resulting in a better waveguiding effect in the corridor, especially with an increase in transmitter height from 1.6 m to 2.3 m.

B. FAST FADING AND SHADOWING

Multiplicative noise arises from median path loss, shadowing and fast fading processes (Fig. 5) that a wave propagated from the transmitter antenna to the receiver antenna suffers in the propagation link. These processes depend on both the relative position of the elements of a wireless system and the obstructions in the channel. Fast fading results from rapid signal variations on the scale of half-wavelength and is often removed by filtering.
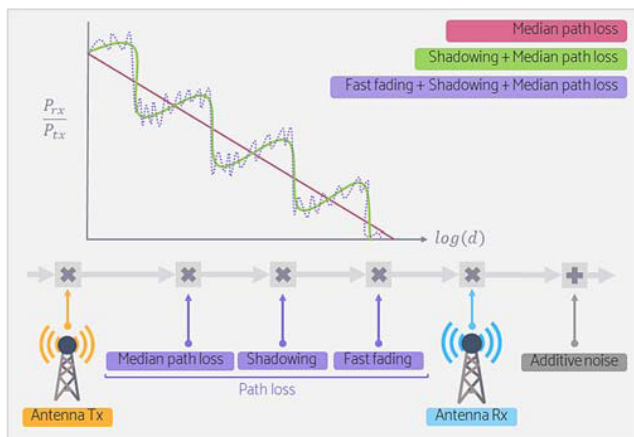

FIGURE 5. Path loss process.

For indoor channels, shadowing occurs due to the large variability of obstructions present in the venue, which results in a received power that fluctuates randomly over time. This behavior is described by a zero-mean log-normally distributed random variable.

Statistical characterization of the received signal variations for both fading and shadowing is useful in the design of transceivers. Thus, knowledge of large-scale variations is

useful in power control techniques and in the evaluation of the coverage service area, as stated in [19].

Common fading models have been characterized in terms of multipath effects related to Nakagami-m, Rayleigh, and Rician distributions [20], [21]. The Fisher-Snedecor F distribution has been recently proposed as a more accurate and mathematically-tractable composite fading model than these traditional established models to describe the combined effects of shadowing and multipath fading in wireless communications [22]–[24]. An example of this is reported in [25], where Yoo *et al.* found that the F distribution can provide a better fit to the experimental data obtained for device-to-device communications within an open office area and an outdoor environment at 5.8 GHz, as compared with the well-established KG model.

C. PARAMETERS AFFECTING RADIO PROPAGATION INSIDE BUILDINGS

According to recommendation ITU-R P.1238-10 [26] propagation impairments in an indoor radio channel are caused mainly by:

- Reflection from, and diffraction around, objects (including walls and floors) within the rooms.
- Transmission loss through walls, floors and other obstacles.
- Channeling of energy, especially in corridors at high frequencies.
- People mobility and objects in the room, including possibly one or both ends of the radio link.
- Temporal and spatial variations of basic transmission loss.
- Multipath effects from reflected and diffracted components of the wave.
- Polarization mismatch due to random alignment of the mobile terminal.

The impact of various parameters affecting radio wave propagation inside buildings is shown in Fig. 6 and is discussed in the next subsections.

1) INDOOR BUILDING GEOMETRY

The extent of coverage inside a building is well-defined by its geometry, and the limits of the building itself affect propagation of signals [26]. The building wall structure frequently has several layers, setting up multipath interference and associated resonances within the structure. These can be analyzed by treating each layer as a section of a transmission line, with a characteristic impedance determined by the wave impedance, the frequency and the angle of incidence [4].

The attenuation introduced by a single layer in the building only slightly reduces the received power. However, the accumulation of such effects has the potential to produce significant radio shadows and may result in other propagation mechanisms affecting in-building radio propagation. Table 2 shows some relevant works that have considered indoor building geometry as a key component to analyze significant effects on propagation.

TABLE 2. Relevant works that consider indoor building geometry.

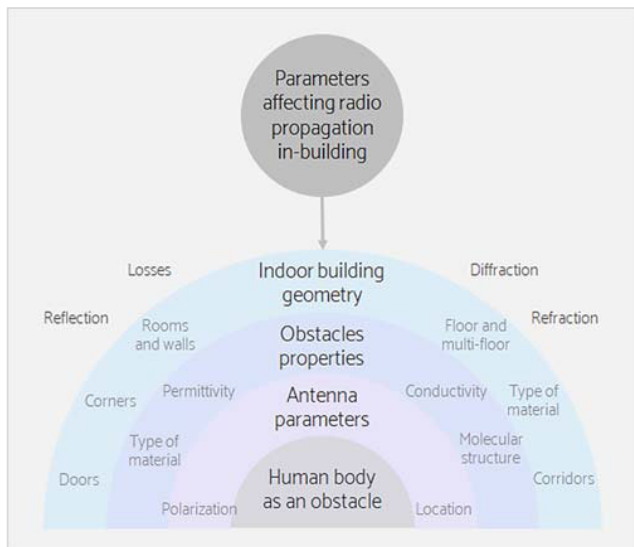| Indoor building	Year	Frequency	Contribution
Glass door; Composite walls (with studs) [28].	2002	60 GHz	Depending on measured received locations through glass door and interior walls showed power losses from 8.8 to 35.5 dB through two composite walls and a loss of 2.5 dB through a glass door. The quantity and position of the metallic studs within the composite wall are important factors to determine the penetration loss.
Inhomogeneous periodic walls [29]	2008	1.0 GHz	Walls are discretized into finite-size building blocks and a finite-difference time-domain (FDTD) approach is used to compute their electromagnetic response in a periodic arrangement as well as in corner and terminal locations.
Glass windows; Drywall; Concrete corners [30].	2011	1.8GHz	When shelves and books are included against internal walls, reflected paths are attenuated to such an extent that diffraction around the corners of the concrete shaft is observed to dominate propagation into the shadow regions. The inclusion of metal window frames perturbs specular reflection from the glass.
Multi-floor [31].	2013	900MHz 2.4GHz	Six different multi-floor building structures that have a stone block type outer wall and are generally described as university, hospital and office type buildings are considered.
Short and long corridors; Wood, glass and mixed doors; Gypsum walls; Textile-wood-glass walls, divisions and metallic cubicles [32].	2018	915MHz	The attenuation in short corridors is lower than in long corridors, with the variation of around 3 dB and peaks up to 7.96 dB.

FIGURE 6. Parameters affecting indoor radio propagation.

permittivity of building materials and of building structures as basic input data (ITU-R P.2040 [27]). Consequently, all possible obstacle properties need to be considered between the transmitter and receiver antenna. In Table 3, some relevant works that take into account these parameters are described in detail.

3) ANTENNA PARAMETERS

A wireless system design aims at delivering optimal signal distribution to all areas inside a building. This power distribution among propagation modes is governed by the position of the transmitter antenna [38]. Over the years, researchers have studied antenna performance and techniques to overcome some restrictions for wireless indoor system design that have been identified, as depicted in Table 4.

For several decades, multiple-input multiple-output (MIMO) antenna technologies have been considered as a promising next-generation technology due to its ability to offer adaptive beamforming gains and spatial multiplexing, substantially increasing capacity for wireless links and especially inside buildings where rich multipath can contribute to higher gains. Therefore, studies that consider this technology have been reported, such as in [39], where the authors survey three new multiple antenna technologies that can play key roles in beyond 5G networks: cell-free massive MIMO, beamspace massive MIMO, and intelligent reflecting surfaces. The advantages of cell-free massive MIMO systems in terms of their energy and cost efficiency are quantified in [40].

4) THE HUMAN BODY AS AN OBSTACLE

The movement of people and objects within a room causes temporal variations of the indoor propagation characteristics. This variation, however, is very slow compared to the

2) OBSTACLE PROPERTIES

The constitutive parameters of building materials are frequency-dependent, even for relatively uniform walls, due to the specific molecular structure of the materials used. For a lossy medium—highly conductive—or for very high frequencies, the skin surface depth is small, thus most of the current stays on the surface of the material and the penetration depth is small. Therefore, a window with metallization will have a high current on its surface near an antenna but will allow little wave penetration. Conversely, even a highly conductive material that is thinner than its skin depth will still allow energy to pass through.

According to ITU-R recommendations, propagation prediction models may need the information on the complex

TABLE 3. Relevant works that consider electromagnetic properties.

Obstacle and property	Year	Frequency	Contribution
▪ Slab wall and complex wall. ▪ Permittivity [33].	2004	90MHz	The patterns of the local mean power distribution for the complex wall cases are quite different from that of the slab and effective wall cases. The areas covered by power contours with same power levels are also different by as much as 40% to 50%.
▪ Single floor. Temperature and relative humidity [34].	2008	2.4 GHz	A direct influence of relative humidity on signal attenuation is identified.
▪ Metallic. ▪ Reflective insulation [35].	2011	70, 200, and 600 MHz	The effects of reflective (metallic) insulation on indoor digital television (DTV) signal reception in rural houses were investigated. Simulation results indicated that under NLOS conditions, the presence of reflective insulation may significantly degrade indoor signal reception and causes a large variation of signal level inside a house.
▪ Solid concrete block wall; Cavity concrete block wall; Red brick wall; Plasterboard wall; Tile roof; Slate roof; Modern windows. ▪ Conductivity; ▪ Thickness [36].	2018	Range from 400 MHz to 2.7 GHz	A maximum attenuation of around 50 dB is observed for windows. Difference in the polarization responses for the windows can be observed. Reasons for the diversity in the results are different composition and structure of the glasses, different metal coating material (conductivity and thickness), and a difference in the number of coated glasses. Due to the largest total thickness, the highest delay is found for cavity concrete block, while the small thickness of slates and plasterboard results in low delay.
▪ Plaster slabs(wall); Aluminum plates (wall). ▪ Permittivity [37].	2019	Range from 26 to 40 GHz	The deduced incident angle highly depends on the material permittivity.

TABLE 4. Relevant works that consider antenna parameters.

Parameter	Year	Frequency	Contribution
Polarization [41].	2007	10.5GHz	Horizontal polarization mitigates the effects of rays reflected from the human body.
Mean effective gain (MEG) [42].	2008	2.1975 GHz	A method is investigated for evaluating the MEG of mobile antennas in LOS street microcells with low base station antennas. The proposed statistical distribution model is valid and effective in both estimating the MEG values of mobile antennas and designing the LOS street microcell systems with low base station antennas.
Location [43].	2008	1800 MHz	Critical regions are identified, where a new transmitter should be placed to provide a better signal for indoor coverage.
Radiation pattern [44].	2013	Range from 2 GHz to 6 GHz	Signal attenuation can be reduced by using antennas with suitable radiation patterns at appropriate locations. While omnidirectional antennas offer better signal coverage in NLOS tunnel regions, directional antennas perform better in LOS regions.
Elevation; Azimuth [45]	2017	2.52 − 2.54 GHz band	The authors provide the elevation and azimuth angular spreads for the measurements done in an urban macro-cellular and urban micro-cellular in an outdoor-to-indoor (O2I) environment and study their dependence on the user equipment (UE) height.
Location; Azimuth angle [18].	2018	14 GHz 22 GHz	Azimuth angle is considered at the receive side, where the directional horn antenna was rotated over azimuth angles in 10° azimuth steps.
Polarization: vertical–vertical (V–V) and horizontal–horizontal (H–H) [36].	2018	Range from 400 MHz to 2.7 GHz	The attenuation introduced by brick (5.24 dB for V–V and 5.54 dB for H–H) and solid block wall (4.32 dB for V–V and 4.36 dB for H–H) is not very significant and there is no advantageous polarization for any of these materials. Plasterboard introduces negligible attenuation with no polarization dependence. Strong polarization dependence of the attenuation is observed with significant transmission losses.
Radiation pattern; MIMO [46].	2020	3 to 4 GHz band	An analysis of the effect that the radiation pattern of the antenna element that makes up the base station array has on the structure of multi-user MIMO channels is presented.

data rate likely to be used and can, therefore, be treated as virtually a time-invariant random variable [26]. Apart from people in the vicinity of the antennas or in the direct path, the people mobility in offices and other locations in and around the building has a negligible effect on propagation characteristics.

TABLE 5. Relevant works that consider human body effects.

Human body effect	Year	Frequency	Accuracy	Considerations
Excess loss due to scattering, blockage and fades due to motion [51]	2006	2.45 GHz	Fading values: 8 dB - 10 dB	Human body shadowing was studied when a person periodically crosses the link about 0.7 m from the receiving antenna for the radio links.
Reflections from body parts [52]	2010	3 - 10 GHz	Standard deviation σ (path loss): 8 dB (PICA) and 6.7 dB (TSA)	The receiver was moved along the front part of the body. Thirty-three different positions were measured on the chest, legs and arms. Two different pairs of planar antennas were used, namely, CPW-fed planar inverted cone antennas (PICA) and miniaturized CPW-fed tapered slot antennas (TSA).
Human body influence depending on specific locations [53]	2010	3.5 GHz	Power level decreases from 2 to 5 dB.	The spectrum analyzer used for measurements supports signaling mode, in which it can be set to record or stop automatically by signals captured, which can be used to reduce the influence of the human body. Despite this, the signaling mode is disabled so the influence of the human body can be investigated.
Body shadowing [54]	2014	900, 1800, 2100 and 2400 MHz	Mean error (path loss): 900 MHz – 0.8 dB, 1800MHz – 1.96 dB, 2100 MHz – 1.49 dB and 2400 MHz -0.56 dB	The body shadowing parameter was computed as the value of mean number of persons per m².
Multiple human body shadowing of multipath [55]	2019	4.7 GHz and 66.5 GHz	The RMS error of the propagation loss estimation model (with human body effects) and the measured value improved by about 1 dB on average	Measurements were performed around a wicket gate of Kamiooka Station, where about 140,000 people passed through it a day. Many human bodies move in the measuring environment, and since there is nothing constructed between the transmitting and receiving sounds, only the human body obstructs the distance between the transmitting and receiving sounds.

Many researchers have quantified the human body effect as an obstacle in radio propagation for indoor. Seesai *et al.* [47], observed that body shadowing leads to lower signal strength and more delay time, directly impacting high data rate applications for signal transmission. When the direct path is shadowed by a person, the attenuation generally increases by more than 20 dB [48]. In the project COST action 231, the authors proposed a stochastic model which reproduces a succession of realistic typical human movements performed in a random manner [49].

Other results confirm that human bodies are significant obstacles (and reflectors) for millimeter-wave propagation (60GHz). The movements within the channel cause a problematic "shadowing effect," especially when the direct path is obstructed. For 2.45, 5.7 and 62 GHz, the propagation channel is at risk from temporal fades caused by people's movement [50], where density and mobility are essential parameters to be considered.

Efforts have been made to develop models that account for human body effects. Ghaddar *et al.* [41] demonstrated that the presence of the human body might be approximated by a conducting circular cylinder at microwave frequencies. To validate the model, vertically- and horizontally-polarized continuous wave measurements were performed at 10.5 GHz between two fixed terminals inside a room along with the presence of an obstacle—person or metallic cylinder—moving along predetermined parallel and perpendicular crossing paths with respect to the LOS direction. Results indicate that there is a strong correlation between the effects of the human body and those of a conducting circular cylinder. Table 5 summarizes characteristics and outcomes

reported in the literature about the indoor path loss models that consider human body effects.

III. INDOOR RADIO WAVE PROPAGATION MODELS

Interference management is at the heart of a suitable wireless propagation prediction, and it is essential for maintaining a desirable throughput while minimizing the impact of interference. The goal of channel modeling is to provide accurate mathematical representations of radio propagation to be used in radio link and system simulations for the system deployment modeling.

In order to meet indoor design demands in an efficient way, many models have been proposed for ensuring system performance, since predictions will be closely related to real values. As a result of this review process, Fig. 7 shows a new classification for indoor channel models, grouping them into two major categories and six subcategories that provide a complete and updated overview. Various types of indoor environments represent hotspot areas to provide radio coverage on public or private buildings, e.g., residential venues, airports, schools, libraries, universities, shopping centers, restaurants, offices, hotels, factories, tunnels, etc. Most of these buildings are considered in the surveyed models and they are reported as target areas in the relevant works stated for empirical, physical, hybrid and outdoor-to-indoor models.

A. GENERAL CASES
1) EMPIRICAL MODELS
These models are based on measurements and observations that are made under different conditions to obtain valuable and building-specific information. Their accuracy depends
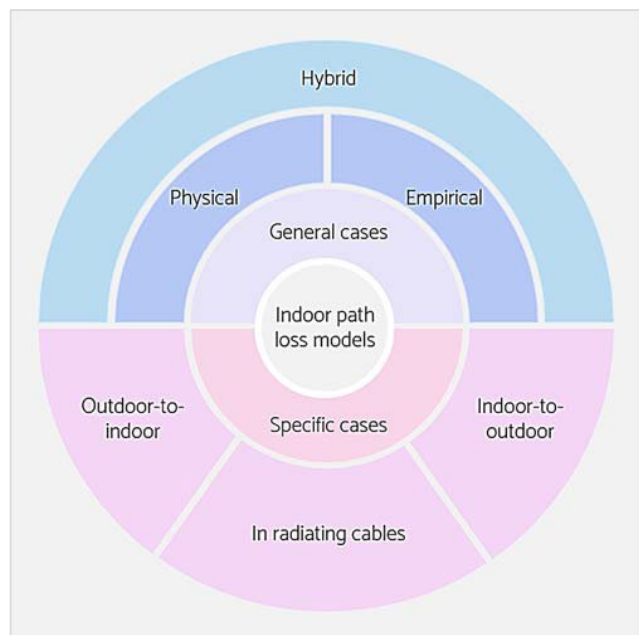
FIGURE 7. Indoor path loss models classification.

not only on the results of measurements but also on the similarity of the environment (measured vs. predicted). Model parameters are tuned with measurements to account for building or site details that otherwise could not be obtained.

Empirical models characterize wave propagation in terms of the distance between transmitter and receiver antenna, operating frequency, antenna heights and angles, number of walls and floors, etc. These models mainly focus on finding path losses from measured data only.

Numerous empirical modeling approaches consider reference models to provide an initial mathematical base, e.g., both the distance power-law model and distance-dependent path loss models are classical references, as the Okumura-Hata is for outdoor. In the case of the distance-dependent path loss model not only the distance between the antennas is taken into account—such as the power-law model [17, Ch. 3]—but also a reference distance (located in the far-field of the radiating antenna [56, Ch. 3]) is considered. Table 6 shows a summary of empirical models published in the literature. Including a specific reference model on each case. Additionally, the standard deviation of the prediction error, σ, is presented as a metric for comparison between measured and modeled data.

According to [32], theoretical models have a high prediction error percentile (average error is the difference between calculated and measured attenuation in [32]), mainly the one-slope model with values between 12% and 27%. Log-distance and ITU models have a better performance for indoor, with different obstacles and corridors considered. An exception for this high error behavior is the empirical model proposed by Morocho-Yaguana *et al.* where the attenuation error is decreased by approximately 10 dB, meaning that the analyzed models have been optimized.

2) PHYSICAL MODELS
Physical models are based on Maxwell's equations to describe the behavior of the electromagnetic field, considering the propagation mechanisms involved. The results provided by physical models are therefore deterministic, i.e., if simulation characteristics remain unchanged the predictions yield the same or very similar results. Although physical models have higher accuracy than empirical, they have the disadvantage of a heavy computational load. Moreover, this high accuracy strongly depends on the accuracy and availability of building databases of the simulated scenarios.

Table 7 summarizes some of the most popular physical models published in the literature, where their principal characteristics are highlighted.

3) HYBRID MODELS
Hybrid models take advantage of the accuracy of physical models and the carefully calibrated radio measurements carried out in empirical models, thus combining the best of both approaches. On this basis, propagation models that combine measurements to adjust parameters that depend on specific building characteristics and consider physical principles for modeling radio wave propagation are known as hybrid models.

According to [26], detailed information of the building structure is necessary for the calculation of indoor field strength, such as in models for indoor prediction based on the uniform geometrical theory of diffraction (UTD) and ray-tracing techniques. These hybrid models combine empirical elements with the theoretical electromagnetic approach of UTD. The hybrid method contemplates direct, single-diffracted and single-reflected rays, and can be extended to multiple diffractions or multiple reflections as well as combinations of diffracted and reflected rays. By including reflected and diffracted rays, the basic transmission loss prediction accuracy is significantly improved.

Table 8 summarizes relevant hybrid indoor models found in the literature.

B. SPECIFIC CASES
1) OUTDOOR-TO-INDOOR (O2I) MODELS
Since 1998, Durgin *et al.* had in mind that measurements and models may aid the development of O2I residential communication wireless systems [84]. The high penetration loss of signals arriving from outdoors limits the range of the covered area inside a building and emphasizes the need for Heterogeneous Networks (HetNet) [85] in providing coverage for obstructed environments.

In accordance with the Small Cell Forum [86], HetNets are defined as "multi-x environment – multi-technology, multi-domain, multi-spectrum, multi-operator and multi-vendor. A HetNet must be able to automate the reconfiguration of its operation to deliver assured service quality across the entire network, and be flexible enough to accommodate changing user needs, business goals and subscriber behaviours". Small

TABLE 6. Relevant works with empirical indoor models.

Model Name	Frequency	Target area	Attenuation	Ref model	Antennas	σ	Considerations
Ericsson Multiple Breakpoint Model (1988) [57]	900 MHz	Business office	Added isolation between the floors of 10dB	Only propagation measurements	-	-	Four breakpoints are included and both an upper and a lower bound on the path loss are considered.
Keenan-Motley Model (1990) [58], [59]	900 - 1700 MHz	Multi storey office construction	6dB per floor	Distance power law model	Rx - Dipole	-	Focuses on the physical properties of walls and floors located between transmitting and receiving antennas.

$$P' + kF = S + 10n \log_{10} d$$

P': Path loss; S: Path loss at 1m, n: power law index, d: distance between transmitter and receiver, F: signal attenuation provided by each floor of the building, k: number of floors traversed.

Model Name	Frequency	Target area	Attenuation	Ref model	Antennas	σ	Considerations
Attenuation Factor Model (1992) [60]	914 MHz	Office building	12.9 dB - 16.2dB per floor	Distance-dependent path loss model	Tx - Omnidirectional quarter-wave monopole Rx – Omni discone	5.8 dB	The effect of building type as well as the variations caused by obstacles are considered.

$$\overline{PL}(d) = PL(d_o) + 10n \log_{10} \left(\frac{d}{d_o}\right) + FAF$$

$$\overline{PL}(d) = 20 \log_{10} \left(\frac{4\pi d}{\lambda}\right) + p \times AF + q \times AF$$

$\overline{PL}$: mean path loss, n: mean path loss exponent, d_o: reference distance, FAF: Floor Attenuation Factor.

p: number of soft partitions, q: number of concrete walls between transmitter and receiver. To predict path loss contours for a transmitter and receiver located in the same wing of an office building where individual office cubicles are separated by cloth-covered plastic dividers).

Model Name	Frequency	Target area	Attenuation	Ref model	Antennas	σ	Considerations
ITU-R Indoor Model (1997) [61]	900 MHz - 100 GHz	Residential; office; commercial	1.8 - 2GHz: residential 4n* dB; office 15+4(n+1) dB; commercial 6+3 (n+1) 900MHz: office: 9dB 1 floor; 19dB 2 floors; 24dB 3 floors;	Distance power law model	-	-	Only floor loss is accounted for explicitly and the loss between points on the same floor is included implicitly by changing the path loss exponent.\n\n*n*: number of floors

$$L_{total} = L(d_o) + N \log_{10} \left(\frac{d}{d_o}\right) + L_f(n)$$

N: distance power loss coefficient, $L(d_o)$: basic transmission loss at 1 m, and assuming free-space propagation $L(d_o) = 20 \log_{10}(f) - 28$ where f is in MHz, L_f: floor penetration loss factor, n: number of floors between base station and portable terminal.

Model Name	Frequency	Target area	Attenuation	Ref model	Antennas	σ	Considerations
Tuan Empirical Indoor Model (2003) [62]	900 MHz - 5.7 GHz	University campus	-	-	Horn directional antennas	6.08 dB at 2.45GHz	Key propagation mechanisms are considered through measurements and key parameters can be tuned using measurements.

$$L = k_1 + G_a + k_2 \log f + k_3 \log R + n_w(k_4 P1 + k_5 P2) + k_6 m_f$$

G_a: antenna gains, f: operational frequency, R: propagation distance, P1 and P2: associate with the angle of incidence to a wall, n_w, m_f: number of walls and floors.

Model Name	Frequency	Target area	Attenuation	Ref model	Antennas	σ	Considerations
Barbosa Indoor Model (2005) [63];	-	5 floors building of a university	-	Distance-dependent path loss model	Rx - monopole	6.05dB	An empirical function (based on Padé approximant) is used, as well as a factor that describes the sign randomness. In [64], the authors employed this model at 2.6 and 3.5 GHz.

$$PL = PL_o + 10\gamma \log_{10} \left(\frac{d}{d_o}\right) + x\sigma + f(n_p, a, b)$$

PL_o: free space propagation from the transmitter to a 1 m reference distance, γ: path loss exponent, x: normalized random variable, σ: standard deviation of the measured data, $f(n_p, a, b)$: function of the number of floors (n_p) between the transmitter and the receiver and of the adjustment parameters a and b.

Model Name	Frequency	Target area	Attenuation	Ref model	Antennas	σ	Considerations
Empirical RMS delay spread model (2017) [65]	2.5 - 2.69 GHz	Indoor stair; corridor; office	-	Distance-dependent path loss model	Tx and Rx - omnidirectional monopole antennas	-	The RMS delay spread is described as a linear function of the path loss, and a normal stochastic variable is introduced.

$$PL(d) = PL(d_o) + 10n \log_{10} \left(\frac{d}{d_o}\right) + C + X_o$$

n: path loss exponent, C: constant, X_o: shadowing effect.

Model Name	Frequency	Target area	Attenuation	Ref model	Antennas	σ	Considerations
Morocho-Yaguana Empirical Model (2018) [32]	915 MHz	University campus	3 dB - 7.96 dB for short (<22m) and long corridors (>22m)	Distance-dependent path loss model	Tx and Rx - Yagi	Average measured attenuation data error of 2.5%	Loss coefficients for structures, shapes, materials and obstacles typical of a campus environment are provided.

$$L_{total} = CF + n \log d + X_o$$

CF: correction factor.

TABLE 7. Relevant works with physical indoor models.

Model Name	Frequency	Target area	Complexity	Ref model	Antennas	σ	Considerations
Honcharenko-Bertoni Model (1992) [66]	852 MHz	Hotel and office building	40 min	Ray optic methods	Validation with measurements using dipole antennas	4.4 dB ($d <$ 30m)	Two principal mechanisms: attenuation due to walls and diffraction from obstacles near the floor and in the plenum, with additional diffraction around the corners, are considered.

$$E_T = \sum_i |E_i|\, e^{-jk\Psi i}$$

ET: total field at a receiving site, Ei: field magnitude, Ψi: phase of the ith ray.

Ray-Tracing Site-Specific Model (1994) [67]	4 and 1.3 GHz	University campus	Parallel computing to allow multiple workstations	Ray-tracing	Tx and Rx - Omnidirectional biconical antennas	<5 dB	Deterministic model that is based on the theory of electromagnetic wave propagation. This algorithm predicts multipath impulse responses based on building blueprints.

$$E_i = E_o f_{ti} f_{ri} L_i(d) \prod_j \Gamma(\theta_{ji}) \prod_k T(\theta_{ki}) e^{-jkd}$$

E_i: complex field amplitude of the ith ray at the receiver, E_o: reference field strength, f_{ti}: field amplitude radiation pattern of the transmitter antenna, f_{ti}: field amplitude radiation pattern of the receiver antenna, $L_i(d)$: path loss distance dependence for the ith multipath component, $\Gamma(\theta_{ji})$: reflection coefficient, $T(\theta_{ki})$: transmission coefficient, e^{-jkd}: propagation phase factor due to path length ($k = 2\pi/\lambda$).

Multichannel Coupling Prediction (2000) [68]	1890 MHz	Office buildings	20 min	Multi-channel Coupling (MCC)	Commercial base station for wireless telephones	-	The MCC method transforms the propagation problem into a linear system of coupled channels. The coupling coefficients that build the interaction matrix of the channels depend only on the geometry of the environment. Once these coupling coefficients are calculated the unknown power in the channels is easily calculated for different transmitter configurations.

$$P_\beta = c_{\alpha\beta} P_\alpha$$

P_β: power leaving the channel β at element A_k, P_α: power leaving at element A_j the channel α, $c_{\alpha\beta}$: energy coming from element A_i reaches element A_k by transmission, reflection or scattering at element A_j.

AZB Algorithm for Efficient Ray Tracing (2000) [69]	950 MHz	Third floor of a building	From 3 h to 10 min by using AZB algorithm	Ray-tracing	-	6.79 dB – 8.33 dB	The Angular Z-Buffer (AZB) model is based on geometrical optics (GO) and the uniform theory of diffraction (UTD).

$$\overrightarrow{E_T}(O) = \{T_\parallel(\theta_i)E_\theta(\theta,\phi)\hat{\theta} + T_\perp(\theta_i)E_\phi(\theta,\phi)\hat{\phi}\}\frac{\exp(-jk_o r)}{r}$$

$\overrightarrow{E_T}$: transmitted field, r: distance between the transmitter antenna and the observation point, $E_\theta(\theta,\phi)$ and $E_\phi(\theta,\phi)$: parallel and perpendicular components of the normalized radiation pattern of the transmitter antenna, θ and ϕ: spherical coordinates of the observation point referred to the coordinate system associated with the antenna, $T_\parallel$ and $T_\perp$: parallel and perpendicular transmission coefficients.

Lee Ray-Tracing Model (2001) [70]	5.2 GHz	University campus	-	Ray launching techniques	Tx - Omnidirectional	-	Propagation effects such as reflection, transmission and diffraction are considered via UTD principles.

$$E_i = E_o f_{ti} f_{ri} L_{fs}(d) \left\{ \prod_f \bar{\bar{R}}_j \prod_k \bar{\bar{T}}_k \prod_l \bar{\bar{D}}_l A_l(s_l, s_l') \right\} e^{-j\beta d}$$

L_{fs}: free space path loss, $\bar{\bar{R}}_j$: reflection coefficient for the jth reflection, $\bar{\bar{T}}_k$: transmission coefficient for the kth transmission, $\bar{\bar{D}}_l A_l$: the diffraction coefficient and the spreading attenuation for the lth diffraction, $e^{-j\beta d}$: propagation phase factor ($\beta = 2\pi/\lambda$ and d represents the unfolded path length).

Ray-tracing model (2019) [71]	5, 31 and 90 GHz	Corridors (University campus)	-	Ray-tracing, close-in free space reference distance (CI) path loss model and the floating-intercept (FI) path loss model	30 and 90 GHz: Directional antennas 5 GHz: Omni-directional antennas	< 2 dB (LOS) < 5 dB (NLOS)	The ray-tracing model X3D in simulation software WI was applied, and the resulting data was post processed and compared with measurement results. Agreement between simulation and measurement results was generally good for average path loss, using both CI and FI models.

$$PL_{CI}(f,d) = FSPL(f,d_o) + 10n \log_{10}\left(\frac{d}{d_o}\right) + X_\sigma{}^{CI}$$

$$PL_{FI}(d) = \alpha + 10\beta \log_{10}(d) + X_\sigma{}^{FI}$$

$FSPL$: free-space path loss at 1 m, $X_\sigma{}^{CI}$: zero mean random variable with standard deviation σ.
α: floating-intercept, β: slope of the line on the log scale, $X_\sigma{}^{FI}$: zero mean random variable.

PGMM model [72]	28 GHz	Indoor conference scenario	-	Normalized power weighted gaussian	*For validation Tx – Omni-directional	-	A normalized power weighted GMM (PGMM) was introduced to model the channel multipath

TABLE 7. *(Continued.)* **Relevant works with physical indoor models.**

				mixture model (PGMM)	Rx Horn antenna		components (MPCs). With MPC power as a weighted factor, the PGMM can fit the MPCs in accordance with the cluster-based channel models.

$$H^{3d}_{n_r,n_t,l} = \sum_{m=1}^{M_t} F^{3d}_{Rx}\left(\theta_{Rx,l}, \phi_{Rx,l}\right) A^{3d}_{l,m} F^{3d}_{Tx}\left(\theta_{Tx,l}, \phi_{Tx,l}\right) e^{j2\pi f_{d,l,m}}$$

$l \in \{1,2,...L\}$, L: number of the clusters, t: time, M_t: number of MPCs in the lth cluster, Tx and Rx: the transmitting and receiving ends, F^{3d}_{Rx} and F^{3d}_{Tx}: transmitting and the receiving antenna responses, $A^{3d}_{l,m}$: polarization matrix, $f_{d,l,m}$: Doppler frequency, n_t and n_r: transmitting and receiving antenna index, $H^{3d}_{n_r,n_t,l}$: sum of the M_t channel MPCs in the lth cluster.

cells—in most cases, for indoor environments—have moved from being a relatively niche technology to fill gaps in coverage and capacity to the central enabler of the emerging HetNet and of 5G. This is the context for the publication of Small Cell Forum's Release 7 [87], which provides a detailed technique for deploying the HetNet and self-optimizing network (SON) and for laying the groundwork for 5G.

SON network functions are widely recognized as key enablers of small cells. Therefore, in the Small Cell Forum's Release 9 [88], the main focus described is SON functionality and performance with special attention to interoperability between small cells and macrocells.

O2I models characterize signal propagation inside buildings coming from an external base station, as illustrated in Fig. 8. O2I modeling becomes very relevant especially in situations where indoor coverage is desired at a reduced cost and capacity demands do not justify the deployment of an indoor cell. A summary of the most important O2I models are stated in Table 9.

FIGURE 9. **I2O specific case.**

FIGURE 8. **O2I specific case.**

Lee *et al.* [89] investigated the multipath dispersion characteristics of O2I propagation in the angular and delay domains. This study is based on field measurement data conducted at 32 GHz in two different office building sites: traditional building and thermally-efficient building.

2) INDOOR-TO-OUTDOOR (I2O) MODELS

Due to the fact that the deployment of femtocells over macrocells—Fig. 9—is currently considered as an attractive solution for extending the coverage area for indoor users, the interference to macrocell subscribers is a key parameter to consider for deploying these systems. To estimate this interference and to consequently ensure optimum network design and operation, studies in propagation I2O models are needed.

In an effort to evaluate the effects of architectural layouts on I2O channels Hamid *et al.* [96] developed a model that can be utilized to characterize this type of channel for femtocell deployments in large buildings—e.g. corporate offices—as well as residential houses. The channel model for the former was performed using exhaustive measurements at an academic facility with a large number of rooms. For the latter, ray-tracing was employed due to the challenges of performing extensive measurements at a statistically large number of different residential houses. By using complementary approaches in [97], Allen *et al.* did not focus their work on characterizing the channel but on facilitating femtocell network deployment through two empirical I2O path loss models derived from continuous-wave (CW) power measurements.

TABLE 8. Relevant works with hybrid indoor models.

Model Name	Frequency	Target area	Ref model	Antennas	σ	Considerations
Reduced-Complexity UTD Model (1998) [73]	900 MHz	University campus	Distance-dependent path loss model; angle-dependent of attenuation factor; UTD	Tx and Rx – omnidirectional antennas	From 20.8 dB (conventional model) to 6.7dB (proposed model)	Additional phenomena suggested by physical models is incorporated in the model, but still the straightforwardness of the empirical approach is retained. The model does not take account of reflected rays.

$$PL_D(d, \phi) = -10 \log \left[\sum_{m=1}^{M} (PL_\angle(d_m) PL_\angle(d'_m) \times |D(d_m, \phi_m, d'_m, \phi'_m)|^2) + PL_\angle(d) \right]$$

M: number of corners in the building database, $D(d_m, \phi_m, d'_m, \phi'_m)$: diffracted fields, (d_m, ϕ_m): coordinates of the corner relative to the transmitter, (d'_m, ϕ'_m) coordinates of the receiver relative to the corner.

Measurement-Based Prediction MbP (2006) [74]	1800 MHz	Old house and modern office building	Distance-dependent path loss model; Keenan–Motley (K&M) model	Tx and Rx – dual-band GSM directional indoor antennas	From 8.43 dB (K&M) to 1.96 dB (MbP)	Path loss is predicted in areas where other indoor models fail to do so. MbP tunes variations with the measurements that are used as part of the modeling process.

$$L_{50} = k_1 + 10n \log r + k_2 r$$
$$L_{50} = L_1 + 20 \log r + n_w a_w + n_f a_f$$

L_{50}: median path loss, k_1 and k_2: parameter to tune using the signal strength measurements, n_w and n_f: number of trespassed walls and floors, a_w and a_f: wall and floor factors to tune.

Hybrid Parabolic Equation-Integral Equation Indoor Model (2007) [75]	2.45 GHz	Indoor scenario (rooms)	Parabolic wave equation (PE)	-	-	No validations

$$\bar{E}_i = \bar{E}_i^0 + \sum_{j=1}^{N} G_{i,j}^B k_0^2 \Delta \varepsilon_j \bar{E}_j S_j$$

$\bar{E}_i^0$: incident electric field, $\Delta \varepsilon_j$: Dielectric constant, $G_{i,j}^B$: Green function, S_j: total surface.

Novel large-scale path loss mode (2015) [76]	28 and 73 GHz	Corridor, open-plan, and closed-plan (research center)	Close-in free space reference distance (CI); floating-intercept (FI) path loss model; alpha-beta-gamma (ABG) model	Tx and Rx – horn antennas	LOS: 10.4 dB (CI) 9.9 dB (CIF) 9.5 dB (ABG) NLOS: 12.5 dB (CI) 11.9 dB (CIF) 11.6 dB (ABG)	The results show that novel large-scale path loss models provided are simpler and more physically-based compared to previous 3GPP and ITU indoor propagation models that require more model parameters and offer very little additional accuracy and lack a physical basis.

$$PL_{CI}(f, d) = FSPL(f, d_o) + 10n \log_{10}\left(\frac{d}{d_o}\right) + X_\sigma^{CI}$$

$$PL_{CIF}(f, d) = FSPL(f, d_o) + 10n \left(1 + b\left(\frac{f - f_o}{f_o}\right)\right) \log_{10}\left(\frac{d}{d_o}\right) + X_\sigma^{CIF}$$

$$PL_{ABG}(f, d) = 10\alpha \log_{10}\left(\frac{d}{d_o}\right) + \beta + 10\gamma \log_{10}\left(\frac{f}{1\ GHz}\right) + X_\sigma^{ABG}$$

b: intuitive model-fitting parameter that represents the slope of linear frequency dependency of path loss, f_o: fixed reference frequency that serves as the balancing point or center of the linear frequency dependency of the path loss exponent (n).
α and γ: coefficients that describe the distance and frequency dependence on path loss, β: optimized offset parameter that is devoid of physical meaning, X_σ^{ABG}: shadowing or large-scale signal fluctuation.

Time-Variant Fading Statistics Model (2015) [77]	3.8 GHz	University campus (office building)	Hidden Markov Model; geometry-based second-order statistics; distance-dependent path loss model	Tx and Rx – custom-made dipole antennas	-	The transitions between the fading states by means of a hidden Markov model parameterized from measurements are characterized. The investigated environment was located on the first floor of an office building and consisted of typical offices along a corridor separated by brick or plasterboard walls.

$$L = \Lambda_0 + \eta \log_{10}\left(\frac{d}{d_o}\right) + \bar{S}$$

Λ_0: deterministic path-loss at the reference distance $d_o = 1$ m, $\bar{S}$: mean shadowing, η: path loss exponent.

TABLE 8. *(Continued.)* **Relevant works with hybrid indoor models.**

Measurement-based spatio-temporal statistical channel model (2015) [78]	60 GHz 70 GHz	Large office rooms, shopping mall, and station scenarios	Power decay and shadow fading model	Tx – Horn antenna Rx – Bicone antenna	$\approx$1 dB (empty office) $\approx$ 2 dB (station scenarios)	The proposed framework covered not only specular but also diffuse signals to provide a complete description of the channel. The validity of the model was demonstrated by means of pathloss and delay spread.

$$\hat{\alpha}_l = P_0 \exp(-\tau_l/\beta_0)\xi$$

P_0: initial pathloss, β_0: power decay factor, ξ: normal random variable, τ_l: delay time.

Optimized Ray Tracing Path Loss Model (2017) [79]	2.4 GHz	Wide corridor	Ray-tracing deterministic N ray model; path loss model (link budget)	Tx - Router Cisco Rx - Tablet	From 11.47 dB (N ray model) to 10.96 dB (modified ray-tracing model)	The accuracy of ray-tracing for estimating the path loss for indoor NLOS propagation is improved using this approach. The ray-tracing model is modified to have a better agreement with measured data.

$$PL_{(nray+Diff+s)} = 10 \log 10 \left(\frac{P_t}{P_{r-nray}}\right) + L_{epstein}(N) + PL_s$$

P_t: transmitted power, P_{r-nray}: received power for an N ray model, $L_{epstein}(N)$: three glass partitions (Epstein Peterson method), PL_s: path loss due to scattering.

Ray-tracing-based simulation (2017) [80]	26 GHz	Center hall (university)	Third dimension (3D) ray-tracing	Tx and Rx – Customized biconical antennas (3 types of virtual antenna array topology MIMO)	Mean error of 3.5 dB	The 3D ray-tracing simulator is calibrated based on the provided indoor measurement results and it is observed that the measurement and the ray-tracing-based simulation results have reached a good agreement.

$$PL = -10 \log_{10}\left(\frac{1}{N_f}\sum_{l=1}^{N_f}|H(f_l)|^2\right)$$

$H(f_l)$: channel transfer function, N_f: number of the measured frequency points.

Extended S-V model (2017) [81]	60 GHz	Office environment	Extended Saleh-Valenzuela (S-V) model	Tx and Rx – horn antennas	-	The measured channel has been modeled based on an angular extended S-V model. The authors found that azimuth departure angles are highly related to antenna position and the measurement environment, while the elevation departure angles are more related to antenna height difference.

$$h(t, \phi_{tx}, \theta_{tx}) = \sum_i A^{(i)} C^{(i)}(t - \mathrm{T}^{(i)}, \phi_{tx} - \Phi_{tx}^{(i)}, \theta_{tx} - \Theta_{tx}^{(i)})$$

$h(t, \phi_{tx}, \theta_{tx})$: Channel impulse response for the channel model in multiple-input single-output, ϕ_{tx} and θ_{tx}: azimuth and elevation angles at the Tx, $A^{(i)}$ and $C^{(i)}$: channel coefficient and channel gain for the ith cluster, $\mathrm{T}^{(i)}, \Phi_{tx}^{(i)}$ and $\Theta_{tx}^{(i)}$: time-angular coordinates of the ith cluster.

Wireless sensor network model (2018) [82]	2.4 GHz and 900 MHz	University campus (laboratory)	Two-ray ground reflection model; distance-dependent path loss model	Tx and Rx – dipole antennas	RMSE: 3.76 (50cm from Tx at 2.4 GHz); 5.05 (50cm from Tx at 900 MHz)	Frequency and three-dimensional link trajectory are considered as key parameters in evaluating path loss. The authors highlighted the effect of height on path loss exponent by means of various measurements taken indoors.

$$PL = 48.64 + 10n \log(f) + 10n \log(d) - n \log(h_t) - n \log(h_r) + X_\sigma$$

h_t and h_r: heights of the transmitter and receiver, X_σ: is determined by studying the theoretical values and the path loss measurements.

mmWave path loss model (2019) [83]	73 GHz	University and airport environments	Close-in reference distance model (CIM); floating-intercept model (FIM)	Tx and Rx – directional horn antenna	-	Results show that the path loss exponent estimated from the CIM is very close to that of the free-space path loss model, while the FIM provides a better fit to the measurement data.

$$PL_{CIM}(d) = PL(d_o) + 10n \log_{10}\left(\frac{d}{d_o}\right) + X_0$$

$$PL_{FIM} = \alpha + 10\beta \log_{10}(d) + X_0$$

$PL(d_o)$: close-in free space path loss, d_o: close-in free space reference distance, X_0: normal random variable with mean 0 dB and standard deviation σ. α: floating intercept, β: linear slope.

TABLE 9. Relevant works with O2I models.

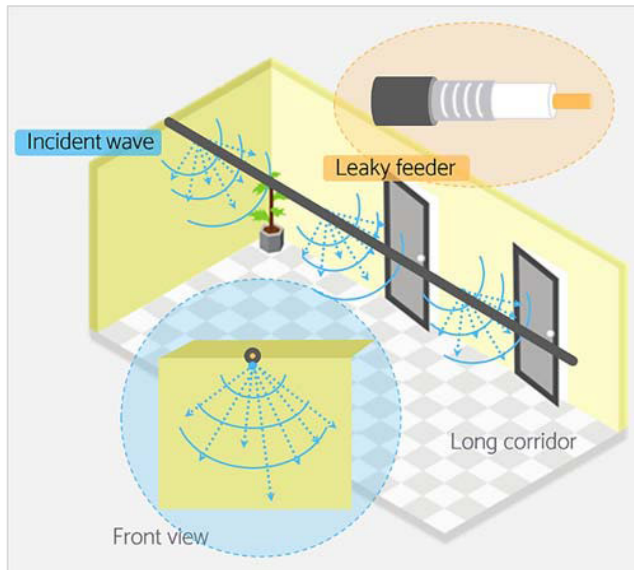| Model Name	Frequency	Target area	Ref model	Antennas	Penetration loss	Considerations
Taga-Miura Model (2002) [90]	8.45 GHz.	Department store	Penetration loss model; loss attenuation model; propagation loss model	Tx - Omnidirectional (d to building <=150m) and directional (d = 300 m)	17.2 dB	The direct path as well as those radio waves propagating through the structural openings along the walls are considered. Measured propagation loss is about 20 dB larger than predicted at positions beyond 120 m.
	$L_p = L_{out} + L_{pn} + L_{in}$ L_{out}: outdoor propagation loss, L_{pn}: building penetration Loss, L_{in}: indoor propagation loss					
Broadband Wireless Access (BWA) Penetration Model (2004) [91]	2.53 and 2.48 GHz	Residential houses; modern apartment complex	COST 231 model; distance-dependent path loss model	-	3 - 3.5 dB (wooden and stucco walls); 1.2 dB (window wall)	The BWA penetration model is based on measurements for various buildings in USA, considering the impact of wall material, angle of incidence and receiver antenna height.
	$L_T = L_{out} + L_e + L_g(1 - \cos v)^2 + n_w L_i$ L_{out}: path loss from the transmitter to the external wall, at the same height as the receiver, L_e: path loss through the external wall at normal incidence ($v = 0$), L_g: additional external wall loss incurred at grazing incidence ($v = \pi/2$), L_i: loss per internal wall, n_w: number of crossed internal walls.					
Ichitsubo–Okamoto Outdoor-to-Indoor Model (2009) [92]	810 MHz, 2.2, 4.7 and 8.45 GHz	Urban area	COST 231 model	Tx and Rx – Dipoles (sleeve antennas)	10 dB *there is no frequency dependence of the penetration loss in the band evaluated	A penetration loss prediction formula is proposed, which is derived from measurements. It is based on measurements of the propagation loss on 71 floors in 17 buildings. RMSE: 7.7 dB
	$\Delta Loss = \alpha \cdot d - G_h \cdot h + \alpha_f \cdot \log(f) + \alpha_{LOS} \cdot LOS + W$ $\Delta Loss$: building penetration loss, d: perpendicular distance to the inside from the nearest window, h: height of the receiver from ground level, W: difference between Loss(out) and Loss(in) at the window, α: penetration distance coefficient (distance attenuation), G_h: floor height gain, α_f: frequency coefficient, α_{LOS}: LOS coefficient.					
Hybrid TDPE/FDTD of Site-Specific Model (2018) [93]	300 MHz	Island environment *Only simulation – no measurements	Time-domain parabolic equation/finite-difference time-domain (FDTD) method	-	-	Through a hybrid time-domain parabolic equation/FDTD method for site-specific venues, radio wave propagation was modeled in a geo-based O2I scenario. Far lower computational cost than with a pure FDTD solution is obtained.
	$u(x, y, z, t) = \sum_{k=0}^{N-1} A(f_k) u(x, y, z, f_k) e^{-i2\pi f_k t}$ $A(f_k)$: Spectrum of the radiating signal, $u(x, y, z, f_k)$: field for the 3-D Parabolic Equation, $e^{-i2\pi f_k t}$: phase factor.					
Statistical O2I Model (2019) [94]	27.85 GHz	University campus	Fourier resolution techniques, measurements	Tx and Rx - phased array antennas. Rx – omni and directional antennas	10.6 − 25.2 dB* strongly depends on the angle of incidence	Statistical models for path loss, delay spread, and angular spread are provided.
Cluster-based model for azimuth/elevation power spectrum APS/EPS (2019) [95]	3.5 GHz	Modern business district	Spatial-temporal channel impulse response (CIR) model	Tx and Rx - array antennas	-	The transmitter was placed on the rooftop of a building to emulate a base station and the receiver was moved in the corridors on different floors in another building to emulate user equipment. Based on measurement results, the lifted-superposed Laplace distribution (LS-Laplace) function and lifted-superposed normal distribution (LS-Normal) function to model the APS and EPS are proposed, respectively.
	$h(\tau, \theta, \phi) = \sum_{l=1}^{L} \alpha_l e^{j\Psi_l} \delta(\tau - \tau_l, \phi - \phi_l, \theta - \theta_l)$ $h(\tau, \theta, \phi)$: spatio-temporal channel impulse response (CIR) model, L: number of signal propagation paths, $\alpha_l e^{j\Psi_l}$: complex gain, τ_l: excess delay, ϕ_l and θ_l: azimuth and elevation angle of the lth path, $\delta(\tau, \theta, \phi)$: n impulse at the excess delay of 0 ns and incident angle of (0°, 0°) in the joint space-and time domain.					

FIGURE 10. Radiating cable used in a building.

When field prediction for indoor base stations or access points is needed both inside and around the building, e.g., for interference assessment and for fingerprinting localization purposes, the model proposed by Degli-Esposti *et al.* in [98] can deliver predictions with good accuracy, based on a combination of a two-parameters propagation formula and a multi-wall model. The model is validated versus both ray-tracing and measurements in different environments, which exhibits good performance in all cases at a small fraction of the ray-tracing computation time.

3) MODELS FOR PROPAGATION IN RADIATING CABLES

Radiating cables or leaky feeders are an alternative solution to provide coverage in challenging enclosed spaces such as tunnels, large corridors or underground mines, as shown in Fig. 10. The cable is leaky, it has gaps or slots in its outer conductor to allow the radio signal to leak into or out of the cable along its entire length, functioning as an extended antenna, making it well adapted to long narrow indoor environments such as corridors, elevators or tunnels [99].

Models for propagating cables have many contributions in wireless systems, some of which are as follows:

- Provide coverage in a small indoor environment: measurements carried out along a corridor in frequencies from 262 MHz to 1226 MHz showed that the leaky feeder is appropriate for coverage in thin indoor environments, which can contribute to the strengthening of the received signal [100].
- Contain signal strength in a better way than a distributed antenna system: in [101], Stamopoulos *et al.* made a comparison of the use of both systems—radiating cable and distributed antenna system (DAS)—to provide coverage in a building and it is clear from their analysis that the radiating cable contains signal strength in a better way than a distributed antenna system. This is due to the characteristics of the radiating cable to provide more

uniformly distributed coverage, avoiding leakage peaks arising from particular antennas in DAS.

- Enable real time localization: in [102] Moschevikin *et al.* and in [103] Serezhina *et al.* studied the possibilities to use leaky feeders also for Time-of-Flight (ToF) based real time localization in such linear topologies, like tunnels, but possibly also for two dimensions (2D) localization. As a general result, leaky feeders might be useful for ToF-based localization using Chirp Spread Spectrum Technologies. However, in [102] they realized that additional signal processing and filtering is required to eliminate the additional variations from the different propagation speeds in the cable and in the air, and the different available propagation paths.

Table 10 summarizes considerations of radiating cable models reported in the literature.

C. INDOOR RADIO PROPAGATION RESEARCH PROJECTS

A general description of COST 231, WINNER II and 3GPP projects are presented below in order to mention the principal projects that were conducted to obtain results about indoor radio propagation modeling.

1) COST 231 [49]

Based on empirical and physical propagation models, the COST 231 project presented adjusted models that were based on propagation measurements, including:

- Empirical models: one-slope model (1SM), multi-wall model (MWM) and linear attenuation model (LAM).
- Physical models: ray launching model (RLM) and image approach method (IAM).
- Frequency: 850, 1800 and 1900 MHz.
- Target areas: office buildings, shopping centers and factories.
- Antennas: Omnidirectional.
- Considerations: the indoor environments were divided into four categories (dense, open, large and corridor) and internal walls are made of thin wood panel.

This model has been suggested in cases where a LOS path exists between a building facade and the external antenna, i.e., single floor propagation. For NLOS, the model relates the loss inside a room to the loss measured outside of it, on the side nearest to the wall of interest, i.e., multi-floor propagation.

Fig. 11 and Fig. 12 summarize the results (standard deviation of prediction error) for the adjusted models taking measurements conducted by Alcatel, TUW and VTT in [49]. The advantage of the MWM and the physical models—IAM and RLM—was most clearly seen in the case when the transmitter and receiver were on different floors. The performance of the 1SM and LAM is poor because they only consider the distance and not the number of penetrated floors.

2) WINNER II [107]

The generic WINNER II channel model follows a geometry-based stochastic channel modeling approach, which allows

TABLE 10. Relevant works with models for propagation in radiating cables.

Model Name	Frequency	Reference model	Penetration loss	σ	Considerations
Zhang Model (2001) [104]	2.0 GHz	Distance power law model; propagation loss (link budget)	9.9 dB (brick wall)	1.88 dB (corridor); 1.98 dB (room)	Coupling and longitudinal losses of the cable are considered. Propagation around the cable termination is not clearly specified.
	$P_r = P_t - \alpha Z - L_c - L_v - L_b - 10n \log_{10} D$ P_r and P_t: received and transmitted power, Z: distance along the cable to the nearest point to the receiver, α: attenuation per unit length of the cable, L_c: coupling loss referenced to 1m radial distance from the cable, L_v: variability in coupling loss, L_b: loss factor due to blockage, D: distance between the cable and the receiver.					
Carter Model (2006) [105]	850 MHz	Friis transmission formula; Keenan-Motley model	5 dB (complex wall)	1.65 dB - 2.14 dB	The radiating cable is modeled as a line source and waves are spread in a cylindrical surface. A radiating cable straight section is considered.
	$S_v(PA, L_{int}, L_v, L_h, f, V_v, x, H, v_f) = PA - L_{int} \cdot L_h + G_v[\theta_v(V_v, L_h, x, H), L_v f, v_f] - L_{ff}[L_v, r_v(H, V_v, L_h, x), f]$ PA: power applied to the driven end of the whole leaky coax run, L_{int}: internal loss of the leaky coax at the frequency f, L_v and L_h: length of the vertical and horizontal segment of the leaky coax, V_v: vertical distance from phone to the midpoint of the vertical leaky coax segment, x: horizontal distance along the leaky coax to the point nearest the phone, H: horizontal distance from phone to closets point of the horizontal segment of leaky coax, v_f: velocity factor of the leaky coax .					
Seseña–Aragón–Castañon Model (2013) [106]	900 - 2500 MHz	Paths from the rays that are perpendicular to cable axis; distance power law model	-	2.2 dB - 4.6 dB	The modeling of some key propagation mechanisms—reflections, refraction losses, radiating cable paths and cable termination—that are present in a practical indoor environment has been incorporated. This model considers situations where there are cable bends and accounts for propagation around the cable termination.
	$P_{r\,Total} = P_r(d_0) + P_r(d_1)R_1 + P_r(d_2)R_2$ R_1 and R_2: empirical coefficients. The distances of reflected signals in walls W_1 and W_2 are d_1 and d_2 respectively. Meanwhile, there is a direct ray that travels from the radiating cable to the receiver where its distance is d_0.					
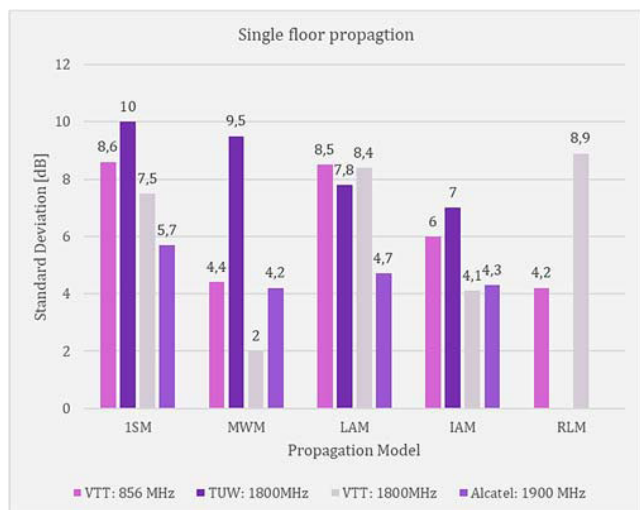
FIGURE 11. Standard deviation of prediction errors for single floor propagation.

FIGURE 12. Standard deviation of prediction error for multi-floor propagation reported by VTT.

the creation of an arbitrary double directional radio channel model. The channel models are antenna-independent, i.e., different antenna configurations and different element patterns can be inserted. The channel parameters are determined stochastically, based on statistical distributions extracted from channel measurements.
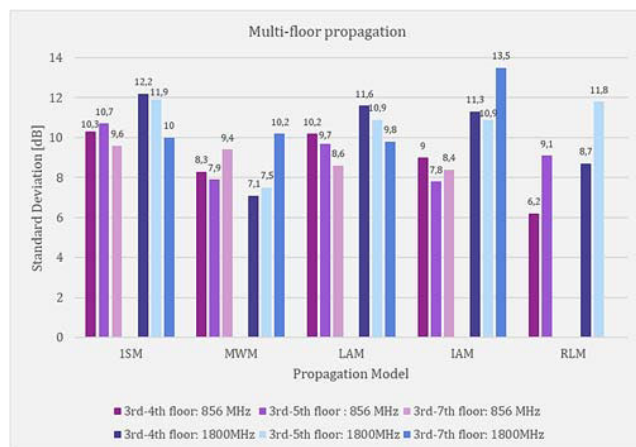
Due to several measurement campaigns carried out in the WINNER II project, the background for the parameterization of the propagation scenarios for LOS and NLOS conditions is provided. The developed models are based on both literature and extensive measurement campaigns. Clustered delay line (CDL) models with fixed large-scale and small-scale parameters were created for calibration and comparison of different simulations. The WINNER II project considered the following characteristics:

- Frequency: 2 – 5 GHz.
- Reference models: 3GPP/3GPP2 spatial channel models and IEEE 802.11n.
- Target areas: indoor office, large indoor hall, indoor-to-outdoor and outdoor-to-indoor scenarios.
- Antennas: different array of antennas.

The path loss models proposed in [107] include four fitting parameters:

- A includes the path-loss exponent.
- B is the path-loss intercept.
- C describes the path loss frequency dependence.
- X is an optional, environment-specific term, e.g., wall attenuation in indoor NLOS scenario).

3) 3GPP

The last technical report about the study on channel model for frequencies from 0.5 to 100 GHz reported by the 3GPP project in [108] considered:

- Reference projects: METIS (Mobile and wireless communications Enablers for the Twenty-twenty Information Society), MiWEBA (Millimetre-Wave Evolution for Backhaul and Access), ITU-R M, COST2100, IEEE 802.11, NYU WIRELESS, Fraunhofer HHI, 5G mmWave Channel Model Alliance, mmMAGIC (Millimetre-Wave Based Mobile Radio Access Network for Fifth Generation Integrated Communications) and IMT-2020 5G promotion association.
- Target areas: office environments, shopping malls and indoor industrial scenarios.

Due to several measurement campaigns carried out in the 3GPPP project, the background for the propagation scenarios for LOS and NLOS conditions is provided. The models proposed are based on measurement campaigns.

Besides, in this report, the path loss incorporating O2I building penetration loss was modeled, taking into account material penetration losses with standard deviations of 4.4 dB for low loss model and 6.5dB for high loss model. The composition of low and high loss is a simulation parameter that should be determined by the user of the channel models and is dependent on the use of metal-coated glass in buildings and the deployment scenarios. Such use is expected to differ in different markets and regions of the world and also may increase over the years due to new regulations and energy-saving initiatives. Furthermore, the use of such high-loss glass currently appears to be more predominant in commercial buildings than in residential buildings in some regions of the world.

The study on channel models reported in [108] took into consideration not only O2I building penetration losses but also O2I car penetration losses, applicable for the frequency range 0.6 - 60 GHz. On the other hand, in [109] the studies have found some extensibility of the existing 3GPP models (e.g. 3GPP TR36.873) to the higher frequency bands up to 100 GHz. Conducted measurements indicated that the smaller wavelengths introduce an increased sensitivity of the propagation models to the scale of the environment and show some
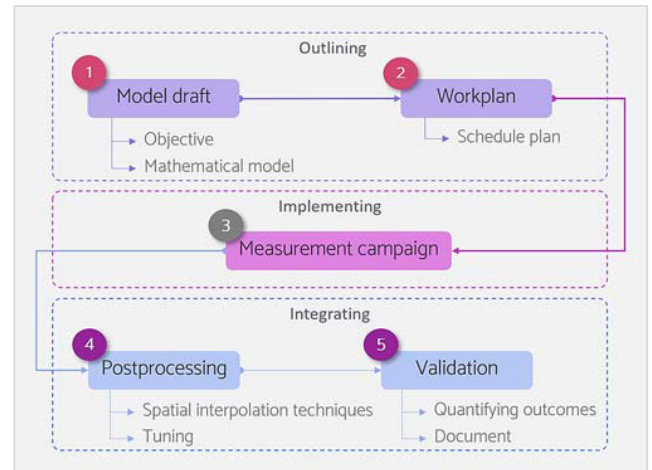
FIGURE 13. Methodology for indoor radio propagation modeling.

frequency dependence of the path loss as well as increased occurrence of blockage. Furthermore, the penetration loss was highly dependent on the material and tended to increase with frequency.

Comparisons of COST-231, WINNER II and 3GPPP projects are shown in Table 11. Some important considerations that have been reported in the literature are indicated. In addition to this, standardization organizations and research institutions have also defined several indoor channel models and recommendations, as summarized in Table 12.

IV. INDOOR CHANNEL MODELING REMARKS

Considering all the features of radio wave propagation models reviewed earlier, accurate path loss predictions as well as available radio measurements are very useful tools for any radio system designer. This section focuses on providing remarks for hybrid models due to the inclusion of theoretical and empirical approaches.

Several issues should be considered as key factors when modeling radio wave propagation indoors. These factors are illustrated in Fig. 13 as a methodology and explained hereafter.

The surveyed studies agree on the way results are presented, i.e., a similar method, which reveals three stages: outlining, implementing and integrating. *Outlining* gives a valuable summary of the model draft and workplan to address the radio wave propagation model approach; *implementing* consists on conducting measurement campaigns to collect all necessary data to complement and to adjust the model; and *integrating* uses previous activities to postprocess and to validate the data obtained from the designed model.

A. OUTLINING
1) MODEL DRAFT

As a first step, the aim of the propagation model should be defined, according to specific requirements. For example, in [43], the authors search for optimal transmitter locations in an indoor wireless system and therefore need a model to achieve this. In [120] the model estimates the optimal

TABLE 11. Comparisons of COST-231, WINNER II and 3GPP projects.

Project	Frequency	Target areas	Considerations
COST-231	850, 1800 and 1900 MHz	Office buildings, shopping centers and factory environments.	▪ Under consideration of a typical O2I model, COST-231 model was the best fit compared to the ray-tracing result at 900, 1800 and 2100 MHz [110]. ▪ In [111] the 3D ray-tracing resulted in an estimation similar to the multi-wall (COST-231) model without requiring a 3D model of the structure or demanding computational power. The 3D ray-tracing generated the best results. however, this advantage is almost negligible over multiwall model which offers a greater simplicity. ▪ COST-231 model can be used as a reasonable lower bound for received power [112].
WINNER II	2 – 5 GHz	Indoor office, large indoor hall, I2O and O2I scenarios.	▪ At 3.5 GHz with an indoor LOS case only WINNER model remains accurate [112]. ▪ In [113], Latinovic et al. demonstrate that WINNER II and similar channel models designed for communications are not suitable, due to: the lack of specular components in los channel, the lack of NLOS bias in NLOS channel and constant delay spread over distance is assumed.
3GPP	0.5 – 100 GHz	Office environments, shopping malls and indoor industrial scenarios.	▪ Delay spread models for O2I scenarios are identical to 3GPP model in both above 6 GHz and below 6 GHz [114]. ▪ The 3GPP models i.e., floating intercept (FI) and alpha-beta-gamma (ABG) models provided reliable performance for path loss for both single and multi-frequency models in LOS scenario at 3.5 GHz and 28 GHz [115].

TABLE 12. Standardization activities about the indoor channel modeling.

Project	Frequency	Target areas	Considerations
ITU-R P.1238-10 [26]	300 MHz to 450 GHz	Residential, office, commercial, factory, corridor, data center, TV studio, computer cluster, classroom, conference room, railway station, airport terminal	▪ Recommendation that provides guidance on indoor propagation mainly general site-independent models and qualitative advice on propagation impairments encountered in the indoor radio environment.
ITU-R M.2135-1 [116]	2 to 6 GHz	Indoor hotspot, O2I	▪ Report that provides guidelines for both the procedure and the criteria (technical, spectrum and service) to be used in evaluating the proposed IMT-Advanced radio interface technologies (RITs) or Sets of RITs (SRITs) for a number of test environments and deployment scenarios for evaluation. ▪ The indoor test environment focuses on isolated cells at offices and/or in hotspot based on stationary and pedestrian users. The key characteristics of this test environment are high user throughput or user density in indoor coverage. ▪ In the O2I case the users are located indoors and base stations outdoors.
IEEE 802.15.4 [117]	100 to 900 MHZ 2 to 10 GHz	Indoor residential, indoor office	▪ Standard that provides models for the UWB channels; it covers indoor residential, indoor office, industrial, outdoor, and open outdoor environments (usually with a distinction between LOS and NLOS properties). ▪ For the frequency range from 100 to 900 MHz, it gives a model for indoor office-type environments.
IEEE 802.15.2 [118]	2.4 GHz	Indoor	▪ Addresses the issue of coexistence of wireless local area networks and wireless personal area networks ▪ Recommends two models for indoor environments where distance is between 0.5 m and 8 m, and greater than 8m.
IEEE 802.11n [119]	2 and 5 GHz	Residential, small office, typical office, large space	▪ Standard that is defined through several specifications of WLANs. It defines an over-the-air interface between a wireless client and a base station or between two wireless clients. ▪ Provides general two-piece distance partitioned model for received signal strength (RSS) behavior for indoor areas. The RSS is modeled as two piecewise linear segments separated by a break point (including LOS and NLOS conditions).

position of fingerprints on an indoor map. Therefore, once the model aim is clear, relevant parameters need to be specified. A decision should be made related to whether the model will be selected from previous research or it will be fully designed, taking into account relevant propagation mechanisms that will be included in the model and thus defining the

corresponding material parameters for a particular building or propagation scenario.

2) WORKPLAN
Planning increases design efficiency and facilitates proper coordination during measurement campaigns, helping to

achieve the objectives of the research. At this stage, radio designers should:

- decide which type of measurements need to be taken; indoor locations to be considered; building features (materials, number of walls and floors, etc.); frequency bands and equipment required;
- carry out a preliminary site visit to contemplate potential test antenna locations and to consider specific building and propagation details;
- evaluate if the campaign requires permission to be granted;
- review technical requirements, i.e., equipment calibration, validation, etc.;
- select proper antenna parameters that will be varied, such as locations, heights, elevation angles, etc.;
- plan the walk test routes to be followed to obtain as much information as possible from the propagation mechanisms and path loss; e.g. Aguirre *et al.*, in [121] reported zig-zag moving pattern through the measurement area to obtain NLOS results;
- estimate the timing to complete the measurement campaign according to time restrictions and granted building permissions;
- choose a suitable navigation to be used indoors, considering that GPS is not available inside buildings; and
- achieve a schedule plan—campaign guide—that includes all previous activities with times and resource descriptions.

According to [122, Sec. 19.8], the most common approach to navigation indoors is called *way-point navigation* and consists of having a digital representation of parts of the building, which may be split by floors or regions. The user interacts with the data collection software where it selects their position at a given point in time on the floor. The software begins recording signal strength samples at regular time intervals from the RF receiver hardware, and data collection continues as the user walks until the end-point on the floor layout is indicated by the user. The collection software then uniformly assigns a position to each discrete sample collected over the period between the start time and end time of the walk segment.

Other indoor navigation systems have been employed and suggested using low-cost stationary sensor nodes. This equipment can be casually placed in the facilities by untrained personnel without location measurement. To acquire knowledge of the physical environment without a map, the system collects radio and compass signatures to continually record paths traversed by users. Using this information, paths are automatically aggregated into path clusters, and a navigable Virtual Roadmap (VRM) of the indoor environment is built by the system [123].

B. IMPLEMENTING
Measurement campaigns are a crucial source of information for in-building radio propagation modeling. On this basis, it is essential to conduct such measurements suitably. Tuning and

validation stages should use different measurement samples from the complete campaign for accurate model design and verification [124], [125]. This involves a dynamic and efficient planning stage—executed in the workplan for efficient implementation.

Once the planning is complete, the measurement campaign is conducted, following the schedule plan for effective radio measurements.

C. INTEGRATING
1) POSTPROCESSING
Postprocessing is employed when signal processing is required to be performed on the raw measured data. Averaging and filtering are common operations performed during post-processing. Postprocessing can be performed in the measured data but also after preliminary predictions have been made, for example, to obtain the local mean of the signal. In this context, it is also used to obtain precise positions of unknown points by relating them to known points. It must be noted that the known points are the result of a previous filter stage, where only useful data is considered (samples that are under the noise floor of the receiver are discarded). After an exhaustive review of indoor modeling, there are two complementary techniques that are contemplated: spatial interpolation and tuning.

When a large amount of useful data is available, model accuracy is greatly improved. However, a small amount of measurements is often available in campaigns due to specific permissions for the selected locations, time restrictions and unreachable places where these measurements cannot be performed. Spatial interpolation techniques show how robust estimates can also be made in such situations, significantly improving the results. The most frequently used techniques, according to [126], are inverse distance weighting (IDW), ordinary kriging (OK) and ordinary co-kriging (OCK).

Kriging is an interpolation technique based on the methods of geostatistics where a subject is concerned with spatial data. Geostatistics assumes that there is an implied connection between the measured data value at a point and where the point is in space. Therefore, it is possible to estimate unknown values from the best set of available sample points.

Thanks to kriging, in [127], Konak created an accurate and complete network coverage map of a target service area from a limited number of test point measurements. Thereby, the cost of time-consuming site surveys can be reduced. Kriging has certain advantages over other interpolation techniques. It is an optimal interpolation method because it produces an unbiased estimate with minimum variance. On the other hand, in [128], several spatial interpolation techniques based on IDW are analyzed and compared in terms of reliability bounds of the interpolation errors for an indoor environment, where performance evaluation shows that the spatial interpolation techniques can provide a robust and reliable estimation data.

TABLE 13. Summary of research opportunities for indoor channel modeling.

Figure of merit	Empirical models	Physical models	Hybrid models
Computational complexity	Low	High	Depends on models selected
Cost	Medium (measurement campaigns)	Low	Medium (measurement campaigns)
Time consumption	Medium	High	Medium – High
Technical resources	Many	Few	Many

When valuable parameters of the mathematical model are tuned from the data obtained in the measurement campaign, the model will be suitable for the actual indoor propagation environment. As reported by Aragón-Zavala [122, Sec. 7.7], the result of model tuning is an optimal trade-off between the benefits and costs of both approaches, saving time and money in the design and implementation.

2) VALIDATION

This process verifies signal strength and coverage predictions made using the model against a set of measurements—only for testing—of the complete campaign. Different estimators for the quantifying validation stage are used. In [18], Oyie and Afullo compared the standard deviation of the signal fluctuation around the mean of the path loss to validate accuracy in predicting path loss. In contrast, in [32] Morocho-Yaguana *et al.* presented a comparative analysis based on the average error, which is the difference between calculated and measured attenuation. The root mean square error (RMSE) is a common estimator for validating the accuracy of a model, as stated in [129]; and the computational complexity is employed for verifying its efficiency.

Finally, it is a good practice to document the survey details, parameters, characteristics, etc. to record the level of accuracy achieved with the indoor radio propagation model. This information may be valuable for future model accuracy comparisons and measurement campaigns.

V. RESEARCH OPPORTUNITIES

The results presented in the works revealed that there are some other sources—techniques—available that could be used to make better in-building predictions, reducing campaign costs and time. Spatial interpolation techniques used for data post-processing can be employed to estimate path loss at unreachable places where measurements cannot be obtained from a limited number of test point measurements conducted at nearby locations, combined with a well-known modeling approach. Future work in this area will take advantage of measurement campaigns, focusing on refining sampling and learning strategies, as well as extracting as much information as possible from existing sources and exploring the trade-off between accuracy and efficacy of the designed model.

The majority of the reviewed work here was predominantly focused in signal strength measurements and propagation properties in two dimensions (2D). However, indoor models that include a third dimension (3D) are scarce, opening research opportunities in the near future.

Model validation at mm-wave frequencies is also required, where more measurements are needed at different venues. Interoperability of various networks and devices with the deployment of 5G networks at various vertical sectors (health, entertainment, transport, intelligent manufacturing, etc.) and the Internet of Things (IoT) will also require novel approaches to model path loss and system performance in more challenging enclosed environments—e.g. factories—to guarantee the required strict grade-of-service levels that this new technology will demand.

Table 13 presents the most relevant research opportunities from the authors' perspective, classified by figure of merit and indoor channel model type.

VI. CONCLUSIONS

The main indoor radio wave propagation characteristics that affect and characterize model performance have been investigated, including path loss, propagation mechanisms, fast fading and shadowing. Additionally, a new taxonomy of indoor channel models has been proposed and analyzed, including an updated overview of indoor channel models. Finally, relevant indoor modeling remarks were established as part of a radio design methodology that includes three stages: outlining, implementing and integrating.

Once the available scientific literature on indoor radio propagation modeling was reviewed, the importance of appropriate modeling become more evident. Small cells are a mainstream element of operators of mobile network deployments for addressing hot-spot areas, in which capacity uplift is needed, such as indoor scenarios, where people spend most of the time. The novel taxonomy proposed herein considers developments which evaluate the effect of indoor small cells over macrocells (I2O models) and the opposite case (O2I models). These models are important specific cases for a HetNet deployment. Besides, general cases are explained as empirical, physical and hybrid models.

The difference between the environment for which the propagation model was developed and the environment for which the model will be used must be carefully evaluated, considering a trade-off between accuracy and efficacy approaches. In physical models, many ray methods are

promising, their accuracy is higher than empirical models but is tied to enough detail of the building geometry and materials. These models are very time consuming, requiring a large computational complexity even for few predictions. In hybrid models, measurement-based methods, rigorous tuning and validation stages are included, taking advantage from empirical and physical models. For these reasons, the choice of the most suitable propagation model approach to be used is mainly driven by specific project requirements, environment, available measurement data, etc. Empirical models can be employed for fast predictions at specific buildings but are strongly dependent on measurement accuracy and can hardly be extrapolated to other buildings, even if they have similar characteristics. Physical models can provide more accurate predictions but until detailed digital building databases and powerful computing resources are readily available, they are still considered inappropriate for most practical designs. It seems that the most promising approach is still the hybrid method, as long as a solid reference model is employed based on physical principles and complemented with accurate measurements to tune relevant parameters.

For the time being, the interested reader which either is new to the field or would like to seek for strong references in narrowband propagation modeling inside buildings can take this paper as a useful guideline.

REFERENCES

[1] *Cisco Visual Networking Index: Forecast and Trends*, Cisco, San Jose, CA, USA, 2019.

[2] *Report to Congress on Indoor Air Quality*, vol. 2. Washington, DC, USA: EPA, 1989.

[3] Small Cell Forum. (2019). *Small Cell Definition*. [Online]. Available: https://www.smallcellforum.org/what-is-a-small-cell/

[4] A. Aragón-Zavala, *Indoor Wireless Communications?: From Theory to Implementation*, 1st ed. Hoboken, NJ, USA: Wiley, 2017.

[5] M. F. Iskander and Z. Yun, "Propagation prediction models for wireless communication systems," *IEEE Trans. Microw. Theory Techn.*, vol. 50, no. 3, pp. 662–673, Mar. 2002.

[6] T. K. Sarkar, Z. Ji, K. Kim, A. Medouri, and M. Salazar-Palma, "A survey of various propagation models for mobile communication," *IEEE Antennas Propag. Mag.*, vol. 45, no. 3, pp. 51–82, Jun. 2003.

[7] K. Anusuya, S. Bharadhwaj, and S. Rani, "Wireless channel models for indoor environments," *Defence Sci. J.*, vol. 58, no. 6, pp. 771–777, Nov. 2008.

[8] A. Neskovic, N. Neskovic, and G. Paunovic, "Modern approaches in modeling of mobile radio systems propagation environment," *IEEE Commun. Surveys Tuts.*, vol. 3, no. 3, pp. 2–12, 3rd Quart., 2000.

[9] D. Trinchero and R. Stefanelli, "Review analysis of electromagnetic modeling methods in confined environments. Part 2: Indoor communications," in *Proc. Int. Conf. Electromagn. Adv. Appl. (ICEAA)*, Sep. 2009, pp. 1070–1073.

[10] P. Smulders, "Statistical characterization of 60-GHz indoor radio channels," *IEEE Trans. Antennas Propag.*, vol. 57, no. 10, pp. 2820–2829, Oct. 2009.

[11] C. Phillips, D. Sicker, and D. Grunwald, "A survey of wireless path loss prediction and coverage mapping methods," *IEEE Commun. Surveys Tuts.*, vol. 15, no. 1, pp. 255–270, 1st Quart., 2013.

[12] A. E. Forooshani, S. Bashir, D. G. Michelson, and S. Noghanian, "A survey of wireless communications and propagation modeling in underground mines," *IEEE Commun. Surveys Tuts.*, vol. 15, no. 4, pp. 1524–1545, 4th Quart., 2013.

[13] A. Hrovat, G. Kandus, and T. Javornik, "A survey of radio propagation modeling for tunnels," *IEEE Commun. Surveys Tuts.*, vol. 16, no. 2, pp. 658–669, 2nd Quart., 2014.

[14] P. Deb, A. Mukherjee, and D. De, "Study of indoor path loss computational models for femtocell based mobile network," *Wireless Pers. Commun.*, vol. 95, no. 3, pp. 3031–3056, Aug. 2017.

[15] I. A. Hemadeh, K. Satyanarayana, M. El-Hajjar, and L. Hanzo, "Millimeter-wave communications: Physical channel models, design considerations, antenna constructions, and link-budget," *IEEE Commun. Surveys Tuts.*, vol. 20, no. 2, pp. 870–913, 2nd Quart., 2018.

[16] S. Ahmadi, "Definition of the performance metrics," in *LTE-Advanced: A Practical Systems Approach to Understanding 3GPP LTE Releases 10 and 11 Radio Access Technologies*. Amsterdam, The Netherlands: Elsevier, 2014, pp. 875–882.

[17] T. S. Rappaport, *Wireless Communications-Principles And Practice*. Upper Saddle River, NJ, USA: Prentice-Hall, 2002.

[18] N. O. Oyie and T. J. O. Afullo, "Measurements and analysis of large-scale path loss model at 14 and 22 GHz in indoor corridor," *IEEE Access*, vol. 6, pp. 17205–17214, 2018.

[19] J. Reig and L. Rubio, "Estimation of the composite fast fading and shadowing distribution using the log-moments in wireless communications," *IEEE Trans. Wireless Commun.*, vol. 12, no. 8, pp. 3672–3681, Aug. 2013.

[20] S. Bhattacharyya, A. Misra, and K. K. Sarma, "A BCH code assisted modified NCO based LSPF-DPLL topology for nakagami-m, Rayleigh and Rician fading channels," *Digit. Commun. Netw.*, vol. 5, no. 2, pp. 102–110, May 2019.

[21] E. Tanghe, W. Joseph, L. Verloock, L. Martens, H. Capoen, K. Herwegen, and W. Vantomme, "The industrial indoor channel: Large-scale and temporal fading at 900, 2400, and 5200 MHz," *IEEE Trans. Wireless Commun.*, vol. 7, no. 7, pp. 2740–2751, Jul. 2008.

[22] H. Du, J. Zhang, J. Cheng, and B. Ai, "Sum of Fisher-Snedecor f random variables and its applications," *IEEE Open J. Commun. Soc.*, vol. 1, pp. 342–356, Mar. 2020.

[23] P. Zhang, J. Zhang, K. P. Peppas, D. W. K. Ng, and B. Ai, "Dual-hop relaying communications over Fisher-Snedecor F-Fading channels," *IEEE Trans. Commun.*, vol. 68, no. 5, pp. 2695–2710, May 2020.

[24] H. Du, J. Zhang, K. P. Peppas, H. Zhao, B. Ai, and X. Zhang, "On the distribution of the ratio of products of Fisher-Snedecor $\mathcal{F}$ random variables and its applications," *IEEE Trans. Veh. Technol.*, vol. 69, no. 2, pp. 1855–1866, Feb. 2020.

[25] S. K. Yoo, S. L. Cotton, P. C. Sofotasios, M. Matthaiou, M. Valkama, and G. K. Karagiannidis, "The Fisher–Snedecor $\mathcal{F}$ distribution: A simple and accurate composite fading model," *IEEE Commun. Lett.*, vol. 21, no. 7, pp. 1661–1664, Jul. 2017.

[26] *Propagation Data and Prediction Methods for the Planning of Indoor Radiocommunication Systems and Radio Local Area Networks in the Frequency Range 300 MHz to 450 GHz*, document P.1238-10, International Telecommunication Union, ITU-R, 2019.

[27] *Effects of Building Materials and Structures on Radiowave Propagation Above About 100 MHz*, document P.2040-1, International Telecommunication Union, ITU-R, 2015.

[28] H. Xu, V. Kukshya, and T. S. Rappaport, "Spatial and temporal characteristics of 60-GHz indoor channels," *IEEE J. Sel. Areas Commun.*, vol. 20, no. 3, pp. 620–630, Apr. 2002.

[29] M. Thiel and K. Sarabandi, "A hybrid method for indoor wave propagation modeling," *IEEE Trans. Antennas Propag.*, vol. 56, no. 8, pp. 2703–2709, Aug. 2008.

[30] A. C. M. Austin, M. J. Neve, and G. B. Rowe, "Modeling propagation in multifloor buildings using the FDTD method," *IEEE Trans. Antennas Propag.*, vol. 59, no. 11, pp. 4239–4246, Nov. 2011.

[31] O. W. Ata, A. M. Shahateet, M. I. Jawadeh, and A. I. Amro, "An indoor propagation model based on a novel multi wall attenuation loss formula at frequencies 900 MHz and 2.4 GHz," *Wireless Pers. Commun.*, vol. 69, no. 1, pp. 23–36, Mar. 2013.

[32] M. Morocho-Yaguana, P. Ludeña-González, F. Sandoval, B. Poma-Vélez, and A. Erreyes-Dota, "An optimized propagation model based on measurement data for indoor environments," *J. Telecommun. Inf. Technol.*, vol. 2, pp. 69–75, Jul. 2018.

[33] Z. Yun, M. F. Iskander, and Z. Zhang, "Complex-wall effect on propagation characteristics and MIMO capacities for an indoor wireless communication environment," *IEEE Trans. Antennas Propag.*, vol. 52, no. 4, pp. 914–922, Apr. 2004.

[34] R. S. De Souza and R. D. Lins, "A new propagation model for 2.4 GHz wireless LAN," in *Proc. 14th Asia–Pacific Conf. Commun. (APCC)*, 2008, pp. 1–5.

[35] J.-B. Yan and J. T. Bernhard, "Investigation of the influence of reflective insulation on indoor reception in rural houses," *IEEE Antennas Wireless Propag. Lett.*, vol. 10, pp. 423–426, 2011.

[36] S. S. Zhekov, Z. Nazneen, O. Franek, and G. F. Pedersen, "Measurement of attenuation by building structures in cellular network bands," *IEEE Antennas Wireless Propag. Lett.*, vol. 17, no. 12, pp. 2260–2263, Dec. 2018.

[37] D. Shi, C. Wang, and Y. Gao, "A new permittivity measurement method for walls in indoor scenes," *IEEE Trans. Antennas Propag.*, vol. 67, no. 4, pp. 2118–2129, Apr. 2019.

[38] Z. Sun and I. Akyildiz, "Channel modeling and analysis for wireless networks in underground mines and road tunnels," *IEEE Trans. Commun.*, vol. 58, no. 6, pp. 1758–1768, Jun. 2010.

[39] J. Zhang, E. Björnson, M. Matthaiou, D. W. K. Ng, H. Yang, and D. J. Love, "Prospective multiple antenna technologies for beyond 5G," *IEEE J. Sel. Areas Commun.*, pp. 1–23, Mar. 2020. [Online]. Available: https://pure.qub.ac.uk/en/publications/prospective-multiple-antenna-technologies-for-beyond-5g

[40] J. Zhang, S. Chen, Y. Lin, J. Zheng, B. Ai, and L. Hanzo, "Cell-free massive MIMO: A new next-generation paradigm," *IEEE Access*, vol. 7, pp. 99878–99888, 2019.

[41] M. Ghaddar, L. Talbi, T. A. Denidni, and A. Sebak, "A conducting cylinder for modeling human body presence in indoor propagation channel," *IEEE Trans. Antennas Propag.*, vol. 55, no. 11, pp. 3099–3103, Nov. 2007.

[42] A. Ando, T. Taga, A. Kondo, K. Kagoshima, and S. Kubota, "Mean effective gain of mobile antennas in Line-of-Sight street microcells with low base station antennas," *IEEE Trans. Antennas Propag.*, vol. 56, no. 11, pp. 3552–3565, Nov. 2008.

[43] A. Dalla'Rosa, A. Raizer, and L. Pichon, "Optimal indoor transmitters location using TLM and Kriging methods," *IEEE Trans. Magn.*, vol. 44, no. 6, pp. 1354–1357, Jun. 2008.

[44] Y. Coulibaly, D. Gilles, H. Nadir, and A. Dodji, "Experimental characterization of the UWB channel for an underground mining vehicle," in *Proc. 7th Eur. Conf. Antennas Propag. (EuCAP)*, 2013, pp. 2331–2334.

[45] V. Kristem, S. Sangodoyin, C. U. Bas, M. Kaske, J. Lee, C. Schneider, G. Sommerkorn, C. J. Zhang, R. S. Thoma, and A. F. Molisch, "3D MIMO outdoor-to-indoor propagation channel measurement," *IEEE Trans. Wireless Commun.*, vol. 16, no. 7, pp. 4600–4613, Jul. 2017.

[46] J. R. Perez and R. P. Torres, "On the impact of the radiation pattern of the antenna element on MU-MIMO indoor channels," *IEEE Access*, vol. 8, pp. 25459–25467, 2020.

[47] W. Seesai, M. Chamchoy, and S. Promwong, "A body-shadowing model for indoor UWB communication environments," in *Proc. 5th Int. Conf. Electr. Eng./Electron., Comput., Telecommun. Inf. Technol. (ECTI-CON)*, vol. 1, May 2008, pp. 261–264.

[48] S. Collonge, G. Zaharia, and G. ElZein, "Influence of the human activity on wide-band characteristics of the 60 GHz indoor radio channel," *IEEE Trans. Wireless Commun.*, vol. 3, no. 6, pp. 2396–2406, Nov. 2004.

[49] *COST Action 231: Digital Mobile Radio Towards Future Generation Systems*, Eur. Commission, Brussels, Belgium, 1999.

[50] F. Villanese, N. E. Evans, and W. G. Scanlon, "Pedestrian-induced fading for indoor channels at 2.45, 5.7 and 62 GHz," in *Proc. IEEE Veh. Technol. Conf.*, 2000, vol. 1, no. 52, pp. 43–48.

[51] A. Kara and H. L. Bertoni, "Effect of people moving near short-range indoor propagation links at 2.45 GHz," *J. Commun. Netw.*, vol. 8, no. 3, pp. 286–289, Sep. 2006.

[52] A. Sani, A. Alomainy, G. Palikaras, Y. Nechayev, Y. Hao, C. Parini, and P. S. Hall, "Experimental characterization of UWB on-body radio channel in indoor environment considering different antennas," *IEEE Trans. Antennas Propag.*, vol. 58, no. 1, pp. 238–241, Jan. 2010.

[53] Z. Lai, N. Bessis, G. de la Roche, P. Kuonen, J. Zhang, and G. Clapworthy, "The characterisation of human body influence on indoor 3.5 GHz path loss measurement," in *Proc. IEEE Wireless Commun. Netw. Conf. Workshops WCNCW*, Apr. 2010, pp. 1–6.

[54] M. Ayadi and A. B. Zineb, "Body shadowing and furniture effects for accuracy improvement of indoor wave propagation models," *IEEE Trans. Wireless Commun.*, vol. 13, no. 11, pp. 5999–6006, Nov. 2014.

[55] M. Nakamura, M. Sasaki, W. Yamada, and Y. Takatori, "Path loss model in crowded indoor environments considering multiple human body shadowing of multipath at 4.7 GHz and 66.5 GHz," in *Proc. 13th Eur. Conf. Antennas Propag. (EuCAP)*, 2019, pp. 1–5.

[56] M. Rahnema, *UMTS Network Planning, Optimization, and Inter-Operation with GSM*. Hoboken, NJ, USA: Wiley, 2008.

[57] D. Akerberg, "Properties of a TDMA pico cellular office communication system," in *Proc. IEEE 39th Veh. Technol. Conf.*, May 1988, pp. 1343–1349.

[58] A. J. Motley and J. M. P. Keenan, "Personal communication radio coverage in buildings at 900 MHz and 1700 MHz," *Electron. Lett.*, vol. 24, no. 12, pp. 763–764, 1988.

[59] J. M. Keenan and A. J. Motley, "Radio coverage in buildings," *Bell Syst. Tech. J.*, vol. 8, pp. 19–24, Jan. 1990.

[60] S. Y. Seidel and T. S. Rappaport, "914 MHz path loss prediction models for indoor wireless communications in multifloored buildings," *IEEE Trans. Antennas Propag.*, vol. 40, no. 2, pp. 207–217, Feb. 1992.

[61] *Propagation Data and Prediction Models for the Planning of Indoor Radiocommunication Systems and Radio Local Area Networks in the Frequency Range 900 MHz to 100 GHz*, document P.1238, International Telecommunication Union, ITU-R, 1997.

[62] S.-C. Tuan, J.-C. Chen, H.-T. Chou, and H.-H. Chou, "Optimization of propagation models for the radio performance evaluation of wireless local area network," in *Proc. IEEE Antennas Propag. Soc. Int. Symp. Held Conjunct, USNC/CNC/URSI North Amer. Radio Sci. Meeting*, vol. 2, Jun. 2003, pp. 146–152.

[63] R. N. S. Barbosa, J. do C. Rodrigues, R. N. S. Barbosa, H. S. Gomes, and G. P. S. Cavalcante, "An empirical model for propagation loss prediction in indoor mobile communications using Padé approximant," in *IEEE MTT-S Int. Microw. Symp. Dig.*, 2005, pp. 625–628.

[64] A. S. Braga, R. L. F. Lopes, S. G. C. Fraiha, J. P. L. Araujo, H. S. Gomes, J. C. Rodrigues, H. R. O. Ferreira, and G. P. S. Cavalcante, "Coverage area simulation for indoor 4G networks in 2.6 GHz and 3.5 GHz," in *Proc. 8th Eur. Conf. Antennas Propag. (EuCAP)*, Apr. 2014, pp. 2125–2129.

[65] Y. Yu, Y. Liu, W.-J. Lu, and H.-B. Zhu, "Measurement and empirical modelling of root mean square delay spread in indoor femtocells scenarios," *IET Commun.*, vol. 11, no. 13, pp. 2125–2131, Sep. 2017.

[66] W. Honcharenko, H. L. Bertoni, J. L. Dailing, J. Qian, and H. D. Yee, "Mechanisms governing UHF propagation on single floors in modern office buildings," *IEEE Trans. Veh. Technol.*, vol. 41, no. 4, pp. 496–504, Nov. 1992.

[67] S. Y. Seidel and T. S. Rappaport, "Site-specific propagation prediction for wireless in-building personal communication system design," *IEEE Trans. Veh. Technol.*, vol. 43, no. 4, pp. 879–891, Nov. 1994.

[68] M. Liebendorfer, M. Zehnder, and U. Dersch, "Multi channel coupling: Interactive prediction of 3D indoor propagation," in *Proc. Int. Zurich Seminar Broadband Commun. Accessing, Transmiss., Netw.*, 2000, pp. 215–221.

[69] F. Saez de Adana, O. G. Blanco, I. Gonzalez Diego, J. P. Arriaga, and M. F. Catedra, "Propagation model based on ray tracing for the design of personal communication systems in indoor environments," *IEEE Trans. Veh. Technol.*, vol. 49, no. 6, pp. 2105–2112, Nov. 2000.

[70] B. S. Lee, "Indoor space-time propagation modelling using a ray launching technique," in *Proc. 11th Int. Conf. Antennas Propag. (ICAP)*, 2001, pp. 279–283.

[71] J. Liu, D. W. Matolak, M. Mohsen, and J. Chen, "Path loss modeling and ray-tracing verification for 5/31/90 GHz indoor channels," in *Proc. IEEE 90th Veh. Technol. Conf. (VTC-Fall)*, Sep. 2019, pp. 1–6.

[72] Y. Li, J. Zhang, P. Tang, and L. Tian, "Clustering in the wireless channel with a power weighted statistical mixture model in indoor scenario," *China Commun.*, vol. 16, no. 7, pp. 83–95, Jul. 2019.

[73] K.-W. Cheung, J. H.-M. Sau, and R. D. Murch, "A new empirical model for indoor propagation prediction," *IEEE Trans. Veh. Technol.*, vol. 47, no. 3, pp. 996–1001, Aug. 1998.

[74] A. Aragon-Zavala, B. Belloul, V. Nikolopoulos, and S. R. Saunders, "Accuracy evaluation analysis for indoor measurement-based radio-wave-propagation predictions," *IEE Microw., Antennas Propag.*, vol. 153, no. 1, pp. 67–74, Feb. 2006.

[75] G. K. Theofilogiannakos, T. V. Yioultsis, and T. D. Xenos, "An efficient hybrid parabolic equation–integral equation method for the analysis of wave propagation in highly complex indoor communication environments," *Wireless Pers. Commun.*, vol. 43, no. 2, pp. 495–510, Oct. 2007.

[76] G. R. Maccartney, T. S. Rappaport, S. Sun, and S. Deng, "Indoor office wideband millimeter-wave propagation measurements and channel models at 28 and 73 GHz for ultra-dense 5G wireless networks," *IEEE Access*, vol. 3, pp. 2388–2424, 2015.

[77] E. Vinogradov, W. Joseph, and C. Oestges, "Measurement-based modeling of time-variant fading statistics in indoor peer-to-peer scenarios," *IEEE Trans. Antennas Propag.*, vol. 63, no. 5, pp. 2252–2263, May 2015.

[78] K. Haneda, J. Järveläinen, A. Karttunen, M. Kyro, and J. Putkonen, "A statistical spatio-temporal radio channel model for large indoor environments at 60 and 70 GHz," *IEEE Trans. Antennas Propag.*, vol. 63, no. 6, pp. 2694–2704, Jun. 2015.

[79] A. Bhuvaneshwari, R. Hemalatha, and T. S. Savithri, "Development of an optimized ray tracing path loss model in the indoor environment," *Wireless Pers. Commun.*, vol. 96, no. 1, pp. 1039–1064, Sep. 2017.

[80] B. Ai, K. Guan, R. He, J. Li, G. Li, D. He, Z. Zhong, and K. M. S. Huq, "On indoor millimeter wave massive MIMO channels: Measurement and simulation," *IEEE J. Sel. Areas Commun.*, vol. 35, no. 7, pp. 1678–1690, Jul. 2017.

[81] X. Wu, C.-X. Wang, J. Sun, J. Huang, R. Feng, Y. Yang, and X. Ge, "60-GHz millimeter-wave channel measurements and modeling for indoor office environments," *IEEE Trans. Antennas Propag.*, vol. 65, no. 4, pp. 1912–1924, Apr. 2017.

[82] M. Abdel-Rahim, M. H. Habaebi, J. Chebil, A. H. A. Hashim, M. M. Ahmed, M. R. Islam, and A. Zyoud, "An indoor path loss model for wireless sensor networks," *Int. J. Ultra Wideband Commun. Syst.*, vol. 3, no. 4, pp. 192–200, 2018.

[83] M. Khatun, C. Guo, L. Moro, D. Matolak, and H. Mehrpouyan, "Millimeter-wave path loss at 73 GHz in indoor and outdoor airport environments," in *Proc. IEEE 90th Veh. Technol. Conf. (VTC-Fall)*, Sep. 2019, pp. 1–5.

[84] G. Durgin, T. S. Rappaport, and H. Xu, "Measurements and models for radio path loss and penetration loss in and around homes and trees at 5.85 GHz," *IEEE Trans. Commun.*, vol. 46, no. 11, pp. 1484–1496, Nov. 1998.

[85] A. Damnjanovic, J. Montojo, Y. Wei, T. Ji, T. Luo, M. Vajapeyam, T. Yoo, O. Song, and D. Malladi, "A survey on 3GPP heterogeneous networks," *IEEE Wireless Commun.*, vol. 18, no. 3, pp. 10–21, Jun. 2011.

[86] *Small Cell Forum*, Small Cell Forum, London, U.K., 2019. [Online]. Available: https://www.smallcellforum.org/

[87] *Small Cell Forum Release 7.0 HetNet and SON Overview*, Small Cell Forum, London, U.K., 2016.

[88] *Small Cell Forum Release 9.0 LTE Small Cell SON Test Cases: Funcionality and Interworking*, Small Cell Forum, London, U.K., 2017.

[89] J. Lee, K.-W. Kim, M.-D. Kim, J.-J. Park, Y. K. Yoon, and Y. J. Chong, "Measurement-based millimeter-wave angular and delay dispersion characteristics of Outdoor-to-Indoor propagation for 5G millimeter-wave systems," *IEEE Access*, vol. 7, pp. 150492–150504, 2019.

[90] Y. Miura, Y. Oda, and T. Taga, "Outdoor-to-indoor propagation modelling with the identification of path passing through wall openings," in *Proc. 13th IEEE Int. Symp. Pers., Indoor Mobile Radio Commun. (PIMRC)*, vol. 1, Sep. 2002, pp. 130–134.

[91] C. Oestges and A. J. Paulraj, "Propagation into buildings for broad-band wireless access," *IEEE Trans. Veh. Technol.*, vol. 53, no. 2, pp. 521–526, Mar. 2004.

[92] H. Okamoto, K. Kitao, and S. Ichitsubo, "Outdoor-to-indoor propagation loss prediction in 800-MHz to 8-GHz band for an urban area," *IEEE Trans. Veh. Technol.*, vol. 58, no. 3, pp. 1059–1067, Mar. 2009.

[93] J. Feng, L. Zhou, X. Xu, and C. Liao, "A hybrid TDPE/FDTD method for site-specific modeling of O2I radio wave propagation," *IEEE Antennas Wireless Propag. Lett.*, vol. 17, no. 9, pp. 1652–1655, Sep. 2018.

[94] C. Umit Bas, R. Wang, S. Sangodoyin, T. Choi, S. Hur, K. Whang, J. Park, C. J. Zhang, and A. F. Molisch, "Outdoor to indoor propagation channel measurements at 28 GHz," *IEEE Trans. Wireless Commun.*, vol. 18, no. 3, pp. 1477–1489, Mar. 2019.

[95] R. Zhang, H. Xu, X. Du, D. Zhou, and M. Guizani, "Dual-polarized spatial–temporal propagation measurement and modeling in UMa O2I scenario at 3.5 GHz," *IEEE Access*, vol. 7, pp. 122988–123001, 2019.

[96] S. Hamid, A. J. Al-Dweik, M. Mirahmadi, K. Mubarak, and A. Shami, "Inside-out propagation: Developing a unified model for the interference in 5G networks," *IEEE Veh. Technol. Mag.*, vol. 10, no. 2, pp. 47–54, Jun. 2015.

[97] B. Allen, S. Mahato, Y. Gao, and S. Salous, "Indoor-to-outdoor empirical path loss modelling for femtocell networks at 0.9, 2, 2.5 and 3.5 GHz using singular value decomposition," *IET Microw., Antennas Propag.*, vol. 11, no. 9, pp. 1203–1211, Jul. 2017.

[98] V. Degli-Esposti, E. M. Vitucci, and R. Martin, "A simple and versatile field prediction model for indoor and indoor-to-outdoor propagation," *IEEE Access*, vol. 5, pp. 13270–13276, 2017.

[99] G. De la Roche and J. Zhang, "Indoor coverage techniques," in *Femtocells: Technologies and Deployment*. Hoboken, NJ, USA: Wiley, 2010, p. 328.

[100] V. P. A. Santos, F. J. B. da Fonseca, L. J. de Matos, W. D. T. Meza, G. L. Siqueira, and L. A. R. Ramirez, "Indoor signal coverage of a leaky feeder cable," in *IEEE MTT-S Int. Microw. Symp. Dig.*, Aug. 2013, pp. 1–5.

[101] I. Stamopoulos, A. Aragon, and S. R. Saunders, "Performance comparison of distributed antenna and radiating cable systems for cellular indoor environments in the DCS band," in *Proc. 12th Int. Conf. Antennas Propag. (ICAP)*, 2004, pp. 771–774.

[102] A. Moschevikin, M. Serezhina, and A. Sikora, "On the possibility to use leaky feeders for positioning in chirp spread spectrum technologies," in *Proc. 2nd Int. Symp. Wireless Syst. Conf. Intell. Data Acquisition Adv. Comput. Syst.*, Sep. 2014, pp. 56–65.

[103] M. Serezhina, A. Moschevikin, R. Evmenchikov, and A. Sikora, "Using radiating cable for time-of-flight CSS measurements indoors and outdoors," in *Proc. IEEE 8th Int. Conf. Intell. Data Acquisition Adv. Comput. Syst., Technol. Appl. (IDAACS)*, vol. 1, Sep. 2015, pp. 91–101.

[104] Y. P. Zhang, "Indoor radiated-mode leaky feeder propagation at 2.0 GHz," *IEEE Trans. Veh. Technol.*, vol. 50, no. 2, pp. 536–545, Mar. 2001.

[105] K. Carter, "Predicting propagation loss from leaky coaxial cable terminated with an indoor antenna," in *Wireless Personal Communications*. Boston, MA, USA: Kluwer, 2006, pp. 71–82.

[106] J. A. Seseña-Osorio, A. Aragón-Zavala, I. E. Zaldívar-Huerta, and G. Castañon, "Indoor propagation modeling for radiating cable systems in the frequency range of 900-2500 MHz," *Prog. Electromagn. Res. B*, vol. 47, no. 47, pp. 241–262, 2013.

[107] P. Kyösti, "IST-4-027756 WINNER II," Wireless World Initiative New Radio, WINNER II Channel Models, Tech. Rep. IST-4-027756 WINNER II D1.1.2 v1.2, 2008.

[108] *Study on Channel Model for Frequencies From 0.5 to 100 GHz*, 3GPP, document TR 38.901, Group Radio Access Network, 2019.

[109] K. Haneda *et al.*, "Indoor 5G 3GPP-like channel models for office and shopping mall environments," in *Proc. IEEE Int. Conf. Commun. Workshops (ICC)*, May 2016, pp. 694–699.

[110] C. Muller, H. Georg, M. Putzke, and C. Wietfeld, "Performance analysis of radio propagation models for smart grid applications," in *Proc. IEEE Int. Conf. Smart Grid Commun. (SmartGridComm)*, Oct. 2011, pp. 96–101.

[111] S. Hosseinzadeh, H. Larijani, K. Curtis, A. Wixted, and A. Amini, "Empirical propagation performance evaluation of LoRa for indoor environment," in *Proc. IEEE 15th Int. Conf. Ind. Informat. (INDIN)*, Jul. 2017, pp. 26–31.

[112] G. Castro, R. Feick, M. Rodriguez, R. Valenzuela, and D. Chizhik, "Outdoor-to-Indoor empirical path loss models: Analysis for Pico and Femto cells in street canyons," *IEEE Wireless Commun. Lett.*, vol. 6, no. 4, pp. 542–545, Aug. 2017.

[113] Z. Latinovic and H. Huang, "A channel model for indoor time-of-arrival ranging," *IEEE Trans. Wireless Commun.*, vol. 19, no. 2, pp. 1415–1428, Feb. 2020.

[114] J. Lee, K.-W. Kim, M.-D. Kim, and J.-J. Park, "32-GHz outdoor-to-indoor channel measurement of propagation losses and delay spread," in *Proc. IEEE Int. Symp. Antennas Propag. USNC-URSI Radio Sci. Meeting (APSURSI)*, Jul. 2019, pp. 2071–2072.

[115] A. M. Al-Samman, T. Abd. Rahman, T. Al-Hadhrami, A. Daho, M. N. Hindia, M. H. Azmi, K. Dimyati, and M. Alazab, "Comparative study of indoor propagation model below and above 6 GHz for 5G wireless networks," *Electronics*, vol. 8, no. 1, p. 44, Jan. 2019.

[116] *Guidelines for Evaluation of Radio Interface Technologies for IMT-Advanced*, document Rep. ITU-R M.2135-1, 2009.

[117] *Standard for Low-Rate Wireless Networks*, IEEE Standard 802.15.4, 2020.

[118] *Coexistence of Wireless Personal Area Networks With Other Wireless Devices Operating in Unlicensed Frequency Bands*, IEEE Standard 802.15.2, 2003.

[119] *Standard for Information Technology—Local and Metropolitan Area Networks*, IEEE Standard 802.11n, 2009.

[120] J. Bi, Y. Wang, Z. Li, S. Xu, J. Zhou, M. Sun, and M. Si, "Fast radio map construction by using adaptive path loss model interpolation in large-scale building," *Sensors*, vol. 19, no. 3, p. 712, Feb. 2019.

[121] S. Aguirre, L. H. Loew, and Y. Lo, "Radio propagation into buildings at 912, 1920, and 5990 MHz using microcells," in *Proc. 3rd IEEE Int. Conf. Universal Pers. Commun.*, Oct. 1994, pp. 129–134.

[122] S. Saunders and A. Aragón-Zavala, *Antenna and Propagation for Wireless Communication Systems*, 2nd ed. Hoboken, NJ, USA: Wiley, 2007.

[123] A. Purohit, Z. Sun, S. Pan, and P. Zhang, "SugarTrail: Indoor navigation in retail environments without surveys and maps," in *Proc. IEEE Int. Conf. Sens., Commun. Netw. (SECON)*, Jun. 2013, pp. 300–308.

[124] D. Plets, W. Joseph, K. Vanhecke, E. Tanghe, L. Martens, S. Bouckaert, I. Moerman, and P. Demeester, "Validation of path loss by heuristic prediction tool with path loss and RSSI measurements," in *Proc. IEEE Antennas Propag. Soc. Int. Symp.*, Jul. 2010, pp. 1–4.

[125] D. Plets, W. Joseph, K. Vanhecke, E. Tanghe, and L. Martens, "Simple indoor path loss prediction algorithm and validation in living lab setting," *Wireless Pers. Commun.*, vol. 68, no. 3, pp. 535–552, Feb. 2013.

[126] J. Li and A. D. Heap, "A review of comparative studies of spatial interpolation methods in environmental sciences: Performance and impact factors," *Ecol. Informat.*, vol. 6, nos. 3–4, pp. 228–241, Jul. 2011.

[127] A. Konak, "A kriging approach to predicting coverage in wireless networks," *Int. J. Mob. Netw. Des. Innov.*, vol. 3, no. 2, pp. 65–71, Jan. 2009.

[128] D. Denkovski, V. Atanasovski, L. Gavrilovska, J. Riihijaervi, and P. Maehoenen, "Reliability of a radio environment map: Case of spatial interpolation techniques," in *Proc. 7th Int. Conf. Cognit. Radio Oriented Wireless Netw. (CROWNCOM)*, 2012, pp. 248–253.

[129] K. Sato, K. Inage, and T. Fujii, "On the performance of neural network residual kriging in radio environment mapping," *IEEE Access*, vol. 7, pp. 94557–94568, 2019.

MELISSA EUGENIA DIAGO-MOSQUERA received the B.Sc. degree in electronics and telecommunications engineering from the University of Cauca, Colombia, in 2014, and the M.Sc. degree in informatics and telecommunications from Icesi University, Colombia, in 2018. She is currently pursuing the Ph.D. degree with the School of Information Technology and Electronics, Tecnológico de Monterrey Campus Querétaro. From 2015 to 2019, she joined the Sugarcane Research Center, CENICAÑA, as a Networks and Telecommunications Engineer facility working on the Internet of Things (IoT) projects, specifically focused on hybrid radiocommunication networks. Her research interests include indoor radio propagation, vehicular technologies, and channel modeling.

ALEJANDRO ARAGÓN-ZAVALA received the B.Sc. degree in electronics and communications engineering from the Tecnológico de Monterrey Campus Querétaro, Mexico, in 1992, the M.Sc. degree in satellite communication engineering from the University of Surrey, U.K., in 1997, and the Ph.D. degree in antennas and propagation from the Centre for Communication System Research, University of Surrey, in 2003. He worked as a Senior In-Building Radio Consultant with Cellular Design Services Ltd., U.K., from 1998 to 2003, and as the Program Chair and the Head of the Electronics Department, Tecnológico de Monterrey Campus Querétaro, from 2003 to 2011. He is currently a Titular Professor and the Head of the Regional Department of Computing, School of Engineering and Science, Tecnológico de Monterrey Campus Querétaro, and a Wireless Expert Consultant with Real Wireless Ltd., U.K. He is the author of more than 40 research articles, two e-books, and three books on wireless communications. His research interests include indoor radio propagation, high-altitude platforms (HAPS), antenna design, vehicular technologies, satellite communications, and channel modeling.

GERARDO CASTAÑÓN received the B.Sc. degree in physics engineering from the Monterrey Institute of Technology and Higher Education (ITESM), Mexico, in 1987, the M.Sc. degree in physics (optics) from the Ensenada Research Centre and Higher Education, Mexico, in 1989, and the master's and Ph.D. degrees in electrical and computer engineering from the State University of New York at Buffalo, in 1995 and 1997, respectively. He was supported by the Fulbright Scholarship through his Ph.D. studies. From 1998 to 2000, he was a Research Scientist with the Alcatel USA Corporate Research Center, Richardson, TX, USA, where he was doing research on IP over WDM, dimensioning and routing strategies for next generation optical networks, and the design of all-optical routers. From 2000 to 2002, he was a Senior Researcher with Fujitsu Network Communications, doing research on ultrahigh speed transmission systems. He has been working with the Department of Electrical and Computer Engineering, ITESM, since 2002. He is an Associate Professor. He has over 90 publications in journals and conferences and four international patents. He frequently acts as a Reviewer for IEEE journals. He is a Senior Member of the IEEE Communications and Photonics Societies. He is a member of the Academy of Science in Mexico and the National Research System in Mexico.

● ● ●